WELCOME…

Metal Fatigue Part 1

Raymond Patin, JSC

Ivatury Raju
ivatury.s.raju@nasa.gov

NESC ACADEMY WEBCAST

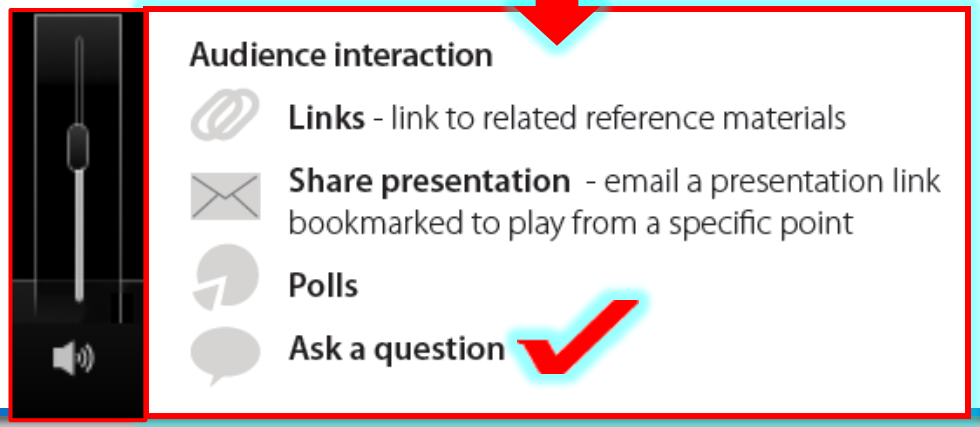

Metal Fatigue

a cursory overview

by

Raymond Patin

NASA/JSC

Subject Outline

- Introduction – Definition & Historical Overview
- The S-N Curve
- The S-N Endurance Limit
- S-N Fatigue Scatter
- Torsion Fatigue
- Mechanics of Fatigue Damage Accumulation
- Fatigue Failure Fracture Surface Features
- Strain-Life
- Linear Elastic Fracture Mechanics
- Fatigue Life Example Problem

Introduction

Structural integrity is a multi-disciplinary endeavor with the objective of preventing catastrophic failures within the operational life of the hardware. Structural integrity is assured via the imposed static strength and service life (fracture control) requirements.

Static Strength

The static strength requirement assures the load carrying capacity of the structure for a single load cycle up to a prescribed maximum load magnitude (limit-load x factor of safety). Static strength verification testing can be performed at various stages (component level, subassembly level, and/or fully integrated assembly) with the inherent assumption that nominal material and build tolerances are captured within the test article. The assumption of a 'nominal material' applies not only to the static strength properties, but also the initial quality regarding preexisting defects that can alter the failure load capacity of the structure. Thus the static strength test article does not verify or define the load carrying capacity of the structure with initial damage and/or structural damage that will accumulate with usage.

Service Life (Fracture Control)

The service life (fracture control) requirements address the time based or usage induced damage mechanisms that degrade the structural load capacity and functionality of the structure. Environmental interactions such as corrosion, mechanical load fluctuations, and/or thermal exposure variations interact to degrade and damage the structure and its load carrying capacity as function of service time. The service life discipline must not only define the rate of damage accumulation, it must also define the load carrying capacity of the structure with damage present (residual strength). Service life verification testing is typically performed on an accelerated time scale which may exclude the time based influences and interactions to some degree. The loss of testing based realism in terms of the time scale, environmental exposures, usage deviations, and boundary condition variations is why usage monitoring and periodic inspections are required to verify service life predictions. The objective of the service life requirements is to define a safe interval of operation with multiple intervention opportunities to mitigate a catastrophic failure in service.

What is metal fatigue?

The definition of "fatigue" according to ASTM* Standard E 1150 reads as follows: "***The process of progressive localized permanent structural damage occurring in a material subjected to conditions that produce fluctuating stresses and strains at some point or points and that may culminate in cracks or complete fracture after a sufficient number of fluctuations***."

***ASTM** – American Society for Testing and Materials

Flow chart description of the metal fatigue process

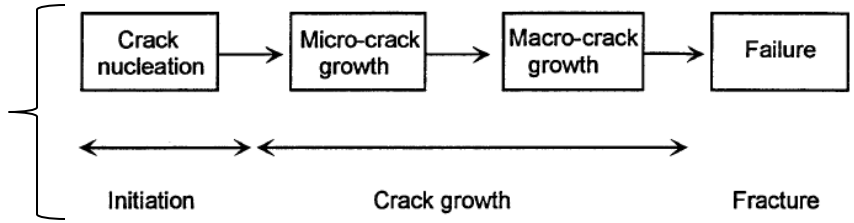

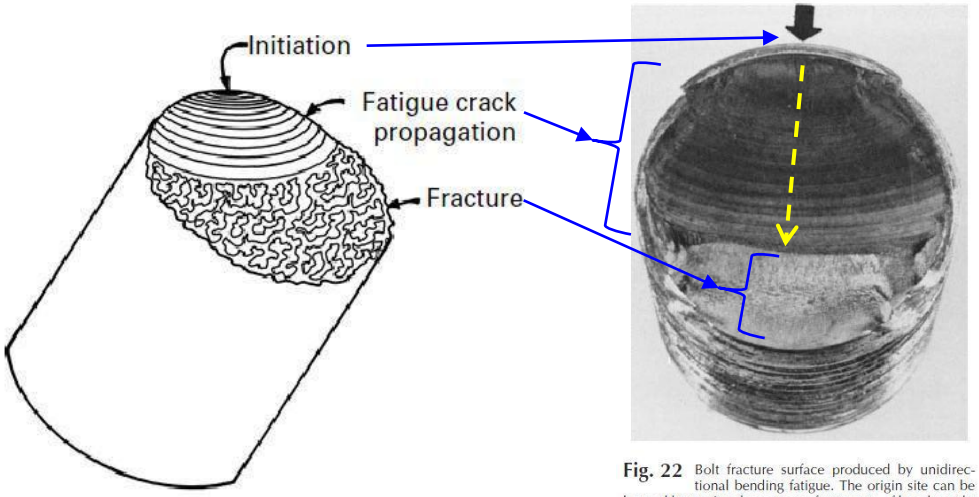

Fig. 22 Bolt fracture surface produced by unidirectional bending fatigue. The origin site can be located by tracing the centers of curvature of beach marks back to the thread root at the arrow. Source: Ref 4

May 8, 1842 – Versailles train crash

An axle of the leading locomotive of a double-headed train suddenly failed (departing King Louis Philippe's birthday celebration), causing it to derail resulting in the second locomotive crashing into the first and the wooden carriages piled into the wreckage where they were set alight by the burning locomotives. More than 75 persons died in the accident. During the subsequent debates regarding the accident the term "fatigue" was coined to describe the sudden fracture of a component from repeated stresses which appeared to be performing well up to that point.

Figure 2 The Versailles accident of 1842 was graphically, if not always accurately, represented contemporary pictures (source Smith, 1990).

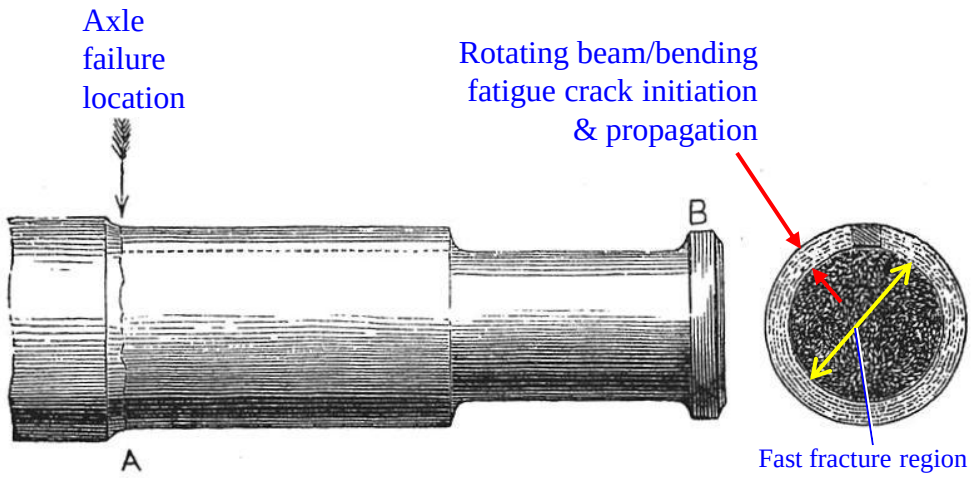

Figure 3 A drawing by Glynn (1844) clearly showing a circumferential crack surrounding the final brittle fracture across a 95 mm diameter section of an axle.

Ref.: R. A. Smith, "**Railways: Structure Integrity, Past, Present, and Future**", Chapter 1.03, *Volume 1, Examples and Case Studies*, R. O. Ritchie and Y. Murakami, volume editors, part of the 10-volume set, ***Comprehensive Structural Integrity***, B. Karihaloo, R. O. Ritchie, and I. Milne, overall editors, Elsevier Science Ltd. Oxford, England, 2003.

The S-N (stress versus life) Curve

The S-N curve : August Wöhler – Rotating Beam Fatigue Testing

In the 1850s and 1860s August Wöhler performed the first systematic laboratory experiments that demonstrate why repeated stresses in railroad axles were so damaging. The rotating beam fixture imposed fully reversed bending stresses over the entire periphery of the specimens. Wöhler was seeking to define the stress level below which an "indefinite" number of reversals could be sustained without failure – defined today as the "endurance limit". Wöhler also demonstrated that applied stress range was more important than stress magnitude.

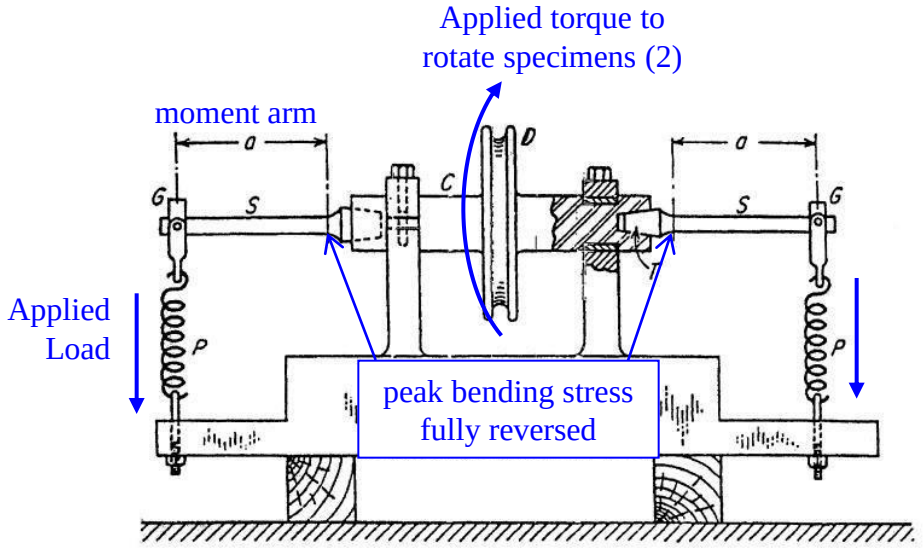

Fig. 3.1 Wöhler's rotating-cantilever, bending fatigue-testing machine. *D*, drive pulley; *C*, arbor; *T*, tapered specimen butt; *S*, specimen; *a*, moment arm; *G*, loading bearing; *P*, loading spring. Source: Ref 3.2

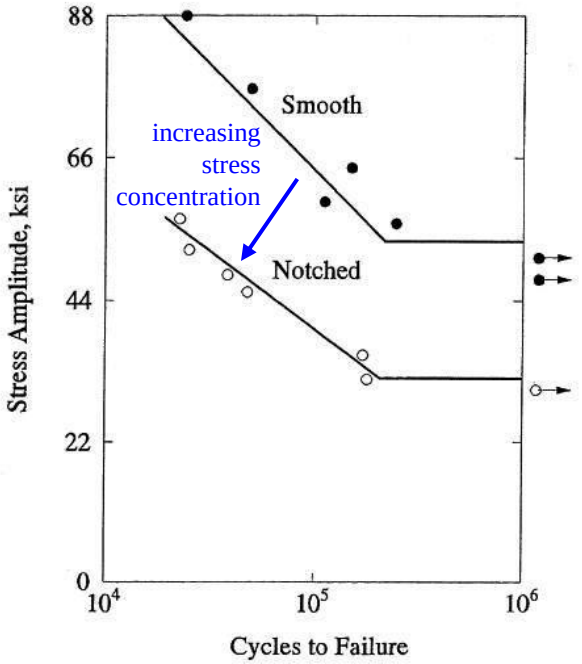

Fig. 3.2 Re-plot of some of Wöhler's data as *S-N* curves for smooth and notched steel specimens

Ref.: S.S. Manson, G.R. Halford, **Fatigue and Durability of Structural Materials**, ASM International, March 2006, pp. 45-46.

The S-N curve : Rotating Beam Fatigue Testing

The linear elastic stress gradient associated with bending results in larger volumes of material being affected as the diameter of the cross section is increased. Larger material volumes at higher cyclic stresses increases the likelihood of microstructural defects being present which adversely impacts fatigue strength. Thus bending fatigue data demonstrates a size effect ; primarily at long lives – less evident in tension fatigue data.

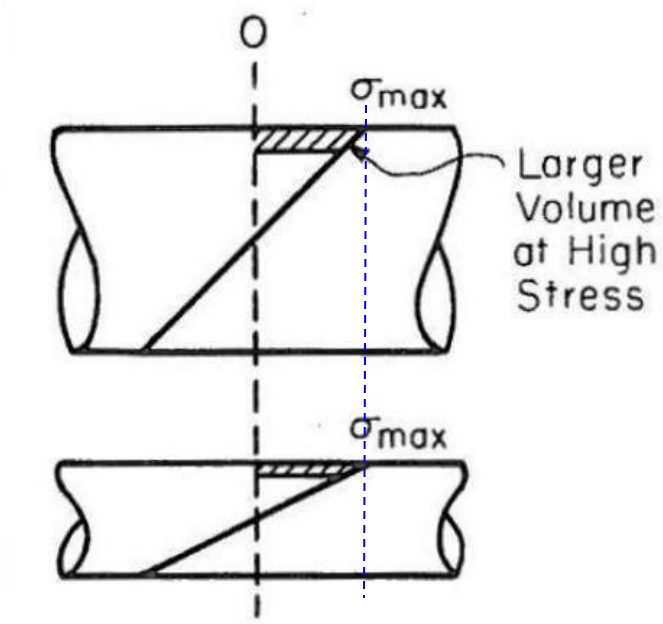

Diameter ↑ → Endurance Limit ↓

TABLE 1.1 Influence of Size on Endurance Limit

Diameter (in)	Endurance Limit (ksi)
0.3	33.0
1.5	27.6
6.75	17.3

Source: J. H. Faupel and F. E. Fisher, *Engineering Design*, John Wiley and Sons, New York, 1981. Reprinted with permission.

Ref.: Bannantine, J., Comer, J., Handrock, J., **Fundamentals of Metal Fatigue**, Prentice-Hall, 1990, pg. 12.

The S-N curve : Linear versus Logarithmic

The same S-N data results are plotted below on a linear and logarithmic scale for the test defined cycles to failure.
The logarithmic scale linearizes the results over a range of applied stress amplitudes.
The Basquin power law relation (1910) defines the finite fatigue life in the linear region ; $S_a = A(N_f)^b$

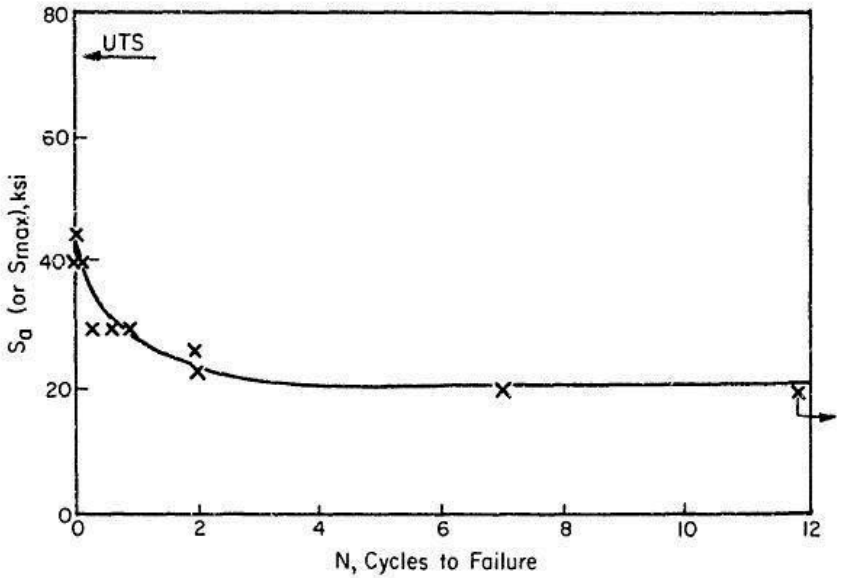

S-N data linear plot

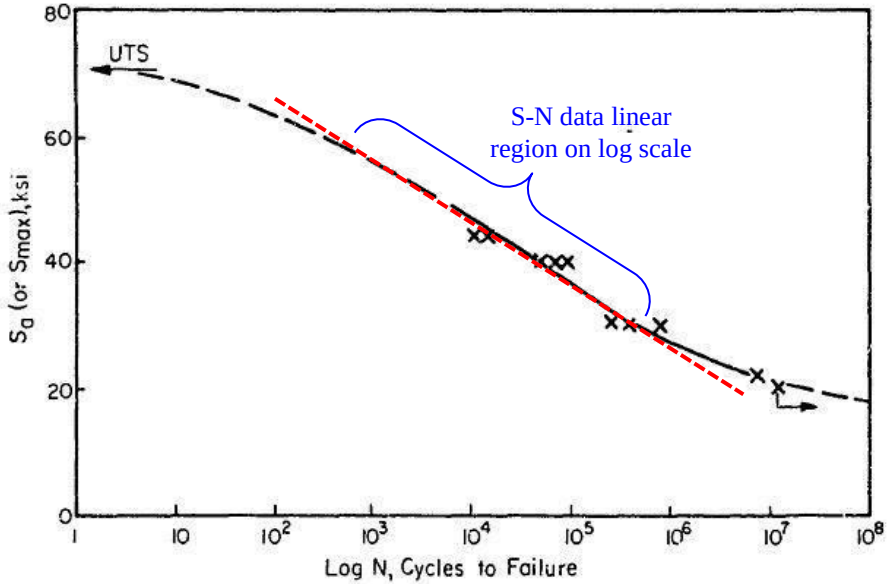

FIGURE 23.—*S–N* curves for 7075–T6 aluminum alloy, fully reversed axial loading.

S-N data logarithm plot

Ref.: Horace J. Grover, **Fatigue of Aircraft Structures, NAVAIR 01-1A-13**, 1960, pg. 36.

Constant Amplitude Cyclic Loading Definition

Constant amplitude cyclic loading is typically utilized for the characterization of materials in fatigue testing. The load-time waveform is typically sinusoidal and varies from a fixed minimum to maximum load magnitude at a defined frequency (cycles/second). *It is noted that most engineering fatigue applications deviate from this simplified loading scheme since the max/min loads vary throughout (variable amplitude loading).*

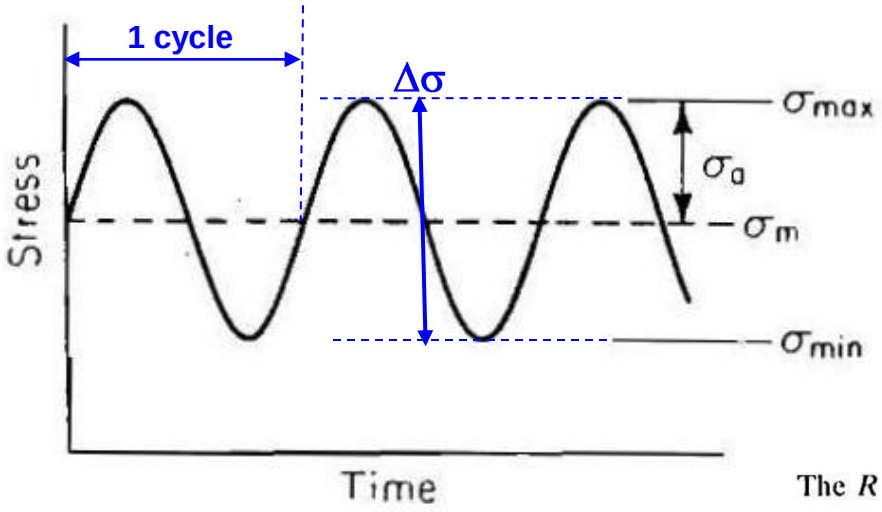

$$\Delta\sigma = \sigma_{max} - \sigma_{min} = \text{stress range}$$

$$\sigma_a = \frac{\sigma_{max} - \sigma_{min}}{2} = \text{stress amplitude}$$

$$\sigma_m = \frac{\sigma_{max} + \sigma_{min}}{2} = \text{mean stress}$$

$$R = \frac{\sigma_{min}}{\sigma_{max}} = \text{stress ratio} \qquad A = \frac{\sigma_a}{\sigma_m} = \text{amplitude ratio}$$

The R and A values corresponding to several common loading situations are:

Fully reversed:	$R = -1$	$A = \infty$
Zero to max:	$R = 0$	$A = 1$
Zero to min:	$R = \infty$	$A = -1$

Ref.: Bannantine, J., Comer, J., Handrock, J., **Fundamentals of Metal Fatigue**, Prentice-Hall, 1990, pp. 5-6.

Stress Ratio Loading Demonstrations

Constant amplitude cyclic loading waveforms for various stress ratio levels are provided below relative to a fixed maximum load/stress ; ($R = \sigma_{min}/\sigma_{max}$) .

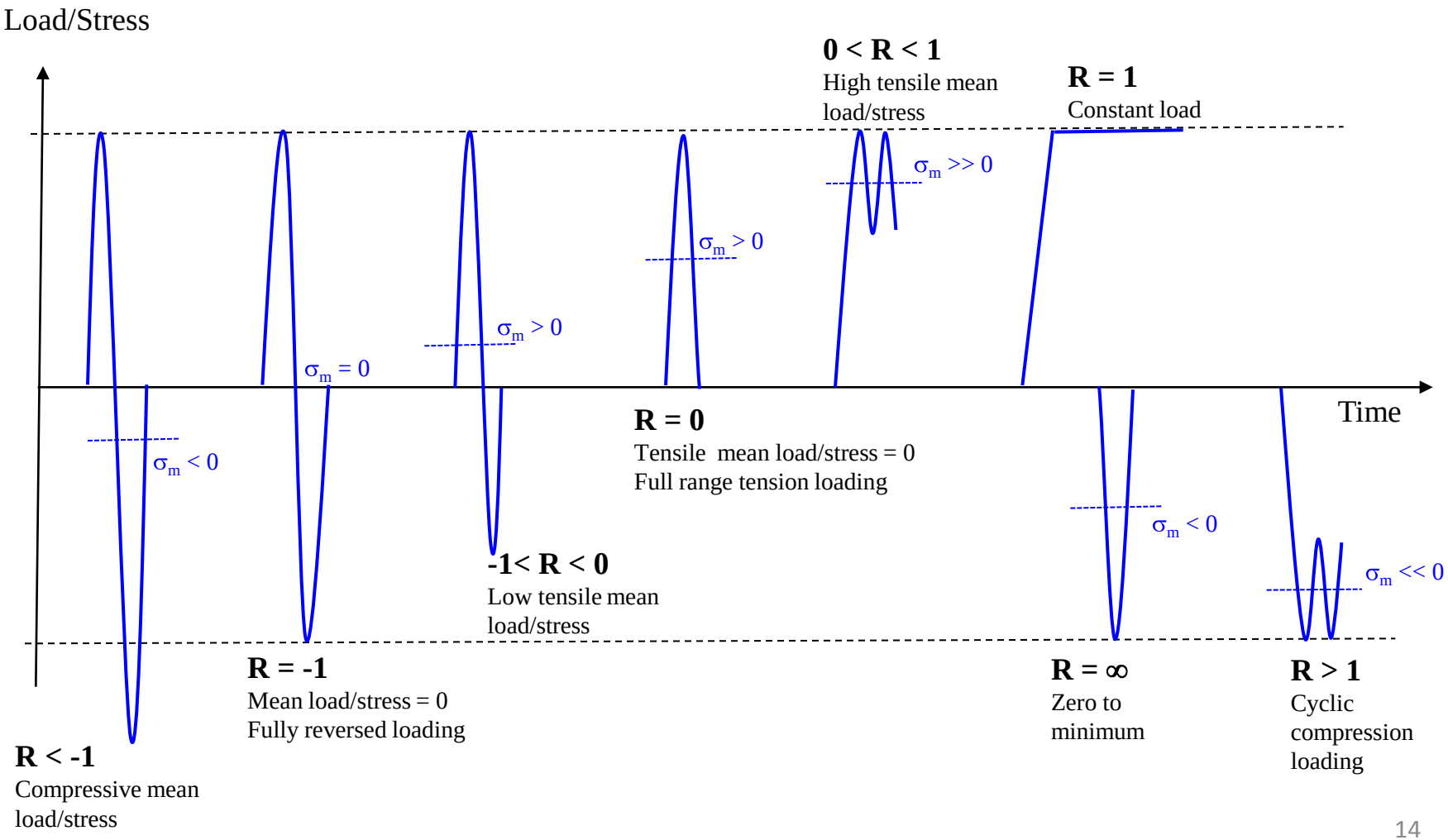

Mean Stress Influence on Constant Amplitude Fatigue Life

The fatigue life is minimized for increasing applied stress ranges ($\Delta\sigma$) at a fixed maximum stress level.
For a fixed alternating stress (σ_a) level the resulting fatigue life will generally decrease within increasing mean stress (σ_m) – applied maximum stress is increasing with increasing mean.

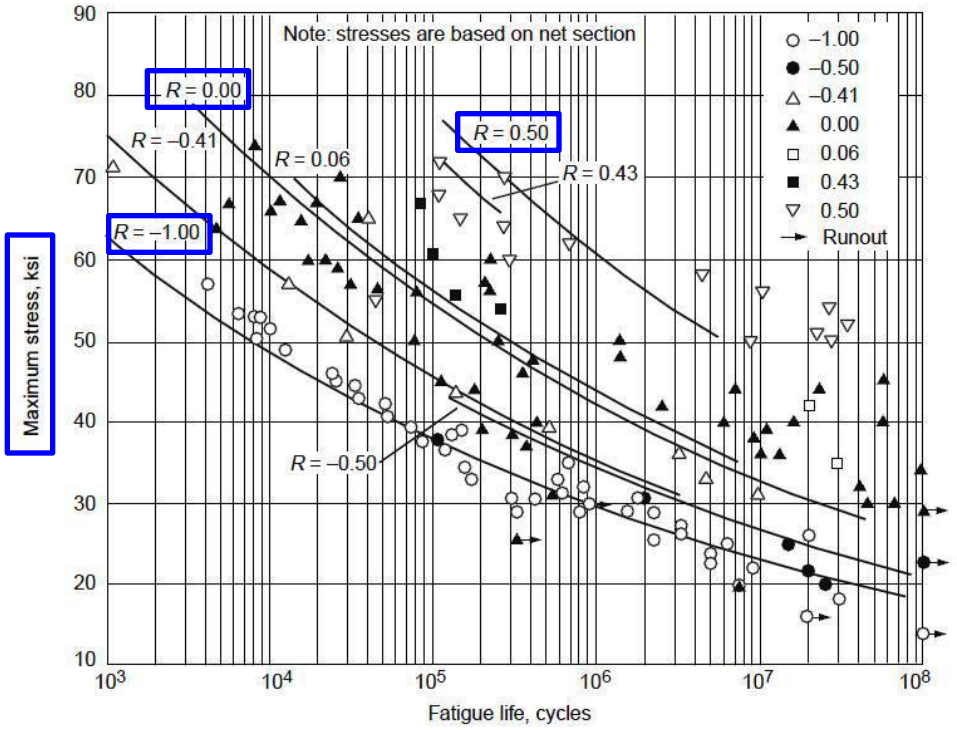

Fig. 2 *S-N* curve for unnotched 2024-T4 aluminum alloy bar. Source: Ref 2

Ref.: **ASM Handbook, Vol. 11 Failure Analysis & Prevention**, Becker, W.T., and Shipley, R.J., editors, ***Fatigue-Life Assessment***, Kaplan, M.P., & Wolff, T.A., pg. 277, ASM International, 2002.

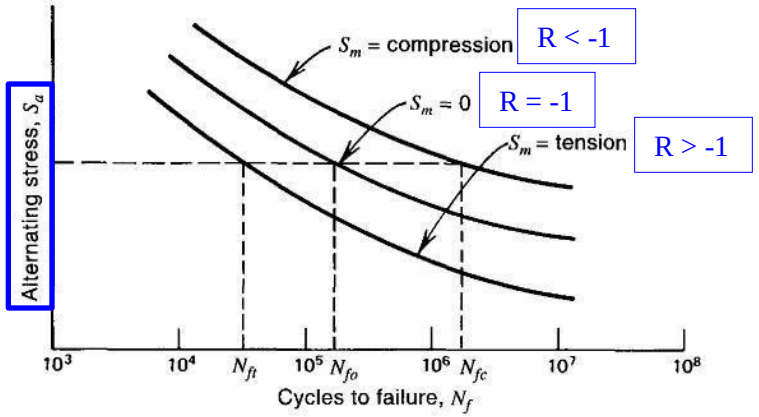

Figure 4.10 Effect of mean stress on fatigue life.

Ref.: Stephens, R.I., Fatemi, A., Stephens, R.R., & Fuchs, H.O., **Metal Fatigue in Engineering, 2nd ed.,** .John Wiley & Sons, 2001, pg 75.

Example of Mean/Residual Stress Influence Limitations

A tensile overload will reverse yield into compression and conversely a compressive underload will reverse yield into tension (for localized yielding enveloped by a large elastic volume). The remaining fatigue life is greater for the compressive residual/mean stress at lower load levels, but the mean stress influence is neutralized at higher load levels by cyclic plastic straining.

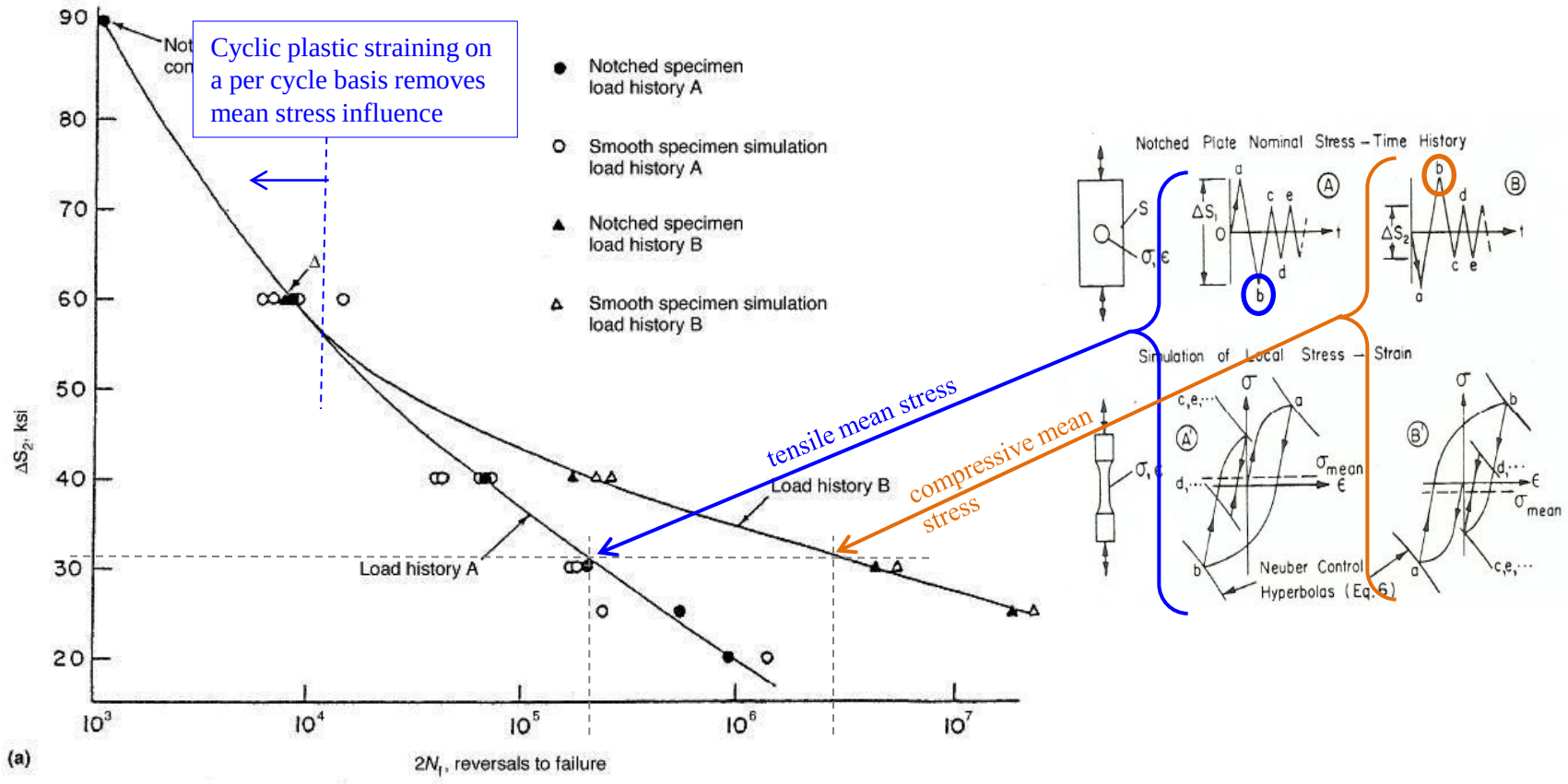

Ref.: Morrow, JoDean, Wetzel, R.M., and Topper, T.H., "**Laboratory Simulation of Structural Fatigue Behavior,**" *Effects of Environment and Complex Load History on Fatigue Life, ASTM STP 462*, 1970, pp. 74-91.

Constant Life (Haigh ; 1917) Diagrams

The S-N fatigue data can be transformed into a constant life diagram as a function of the applied alternating and mean stresses via the test data points at specified cycles to failure. The resulting plot is known as a Haigh diagram (1917) which is used to characterize constant amplitude fatigue data mean stress influences.

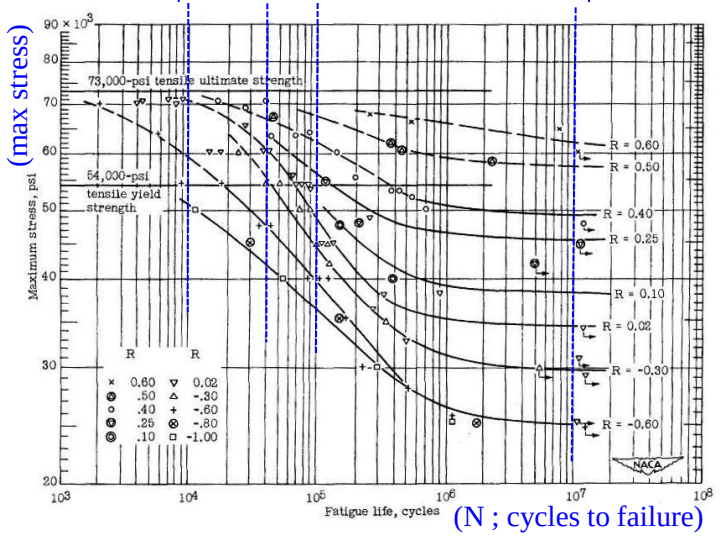

Figure 8.- Results of fatigue tests at 1100 cycles per minute on 24S-T3 aluminum alloy.

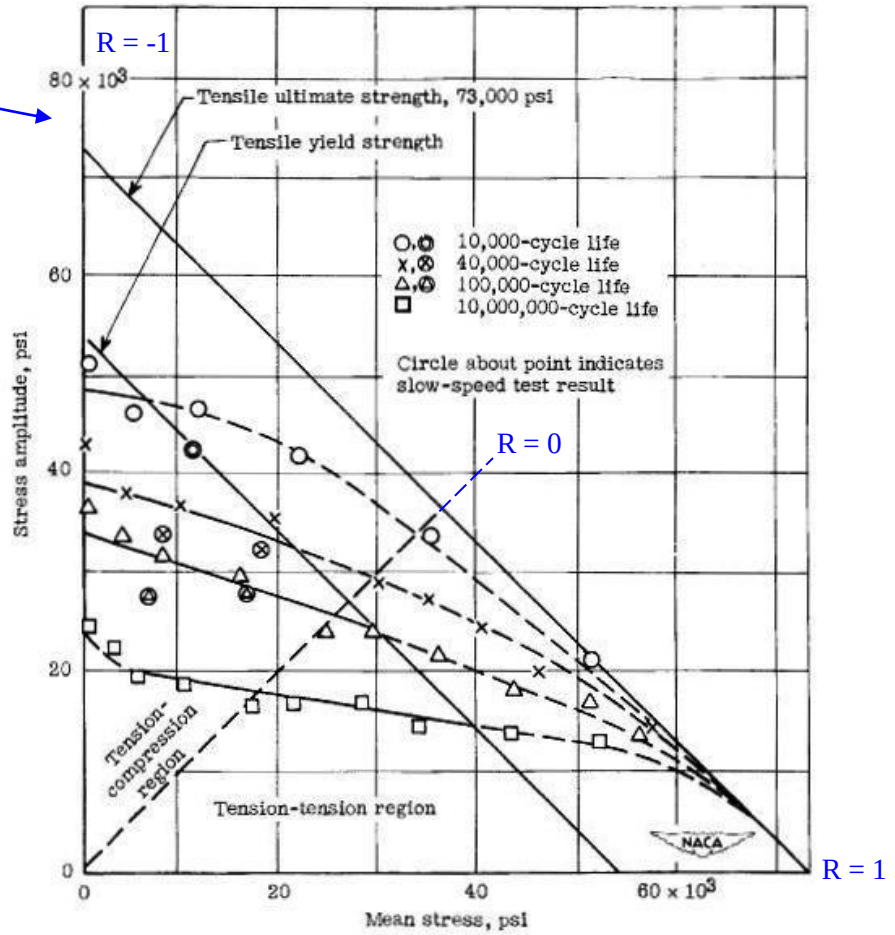

Figure 21.- Constant-lifetime curves, amplitude against mean stress, for 24S-T3 aluminum alloy (see Discussion of Results).

Ref.: Grover, H.J., Bishop, S.M., and Jackson, L.R., NACA TN 2324, March 1951, pp. 51,64.

Master Diagrams

The addition of an extra set of axes (maximum & minimum stress) to the constant life (Haigh) diagram results in a master diagram.

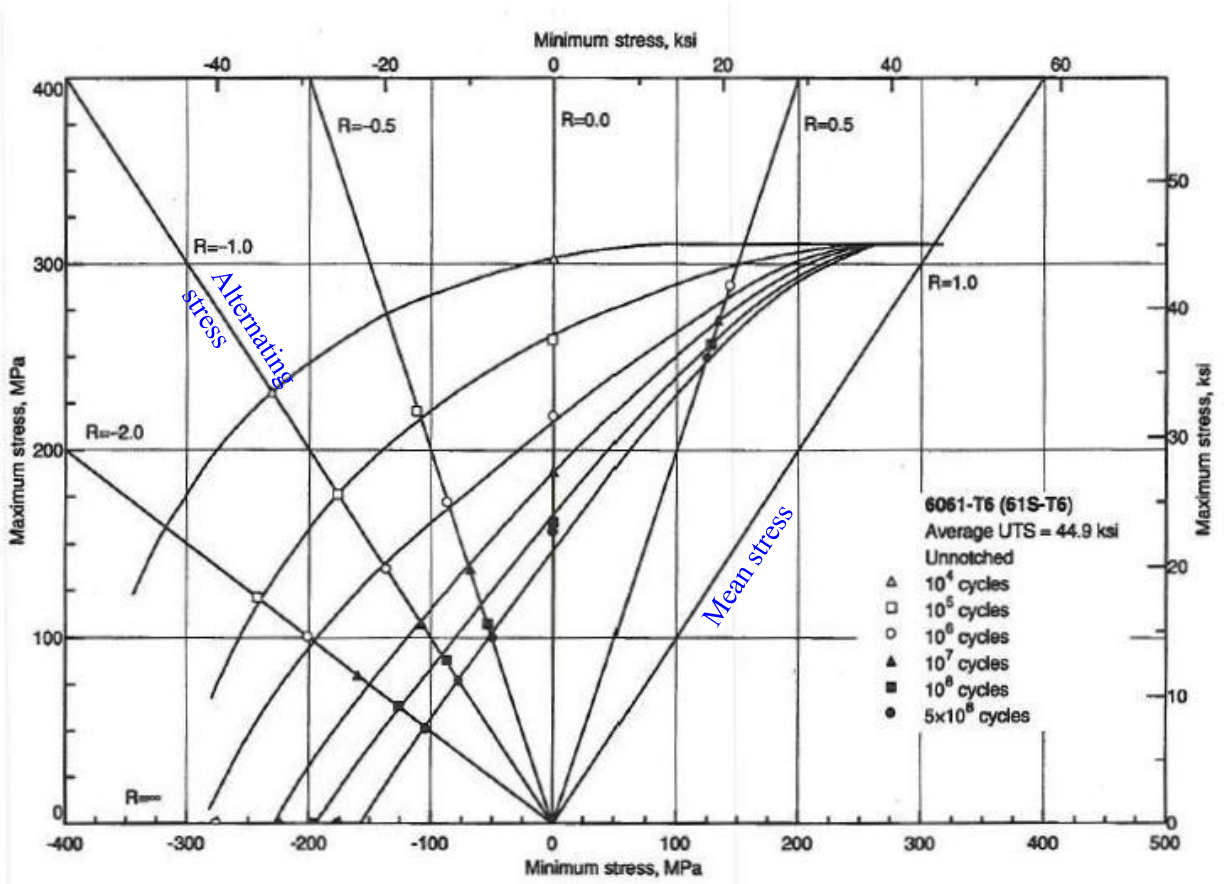

Fig. 72 6061-T6 (61S-T6) unnotched axial fatigue. Source: Alcoa

Ref.: **Fatigue Data Book : Light Structural Alloys,** ASM International, 1995, pg 72.

Goodman Diagram (1899)

The original Goodman diagram (1899) defined the influence of mean and alternated stresses on the resulting cycles to failure with Wohler's data with linear projections as a function of material ultimate strength and applied mean and alternating stresses. A subsequent correction (inclusion of endurance limit) to improve agreement with data results in the modified Goodman equation/diagram.

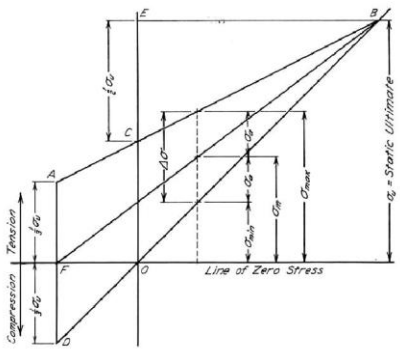

FIG. 2. GOODMAN DIAGRAM SHOWING EFFECT OF RANGE OF NORMAL STRESS UPON ENDURANCE LIMIT

$$\sigma_a = \frac{1}{3}\sigma_u\left(1 - \frac{\sigma_m}{\sigma_u}\right).$$

Goodman diagram

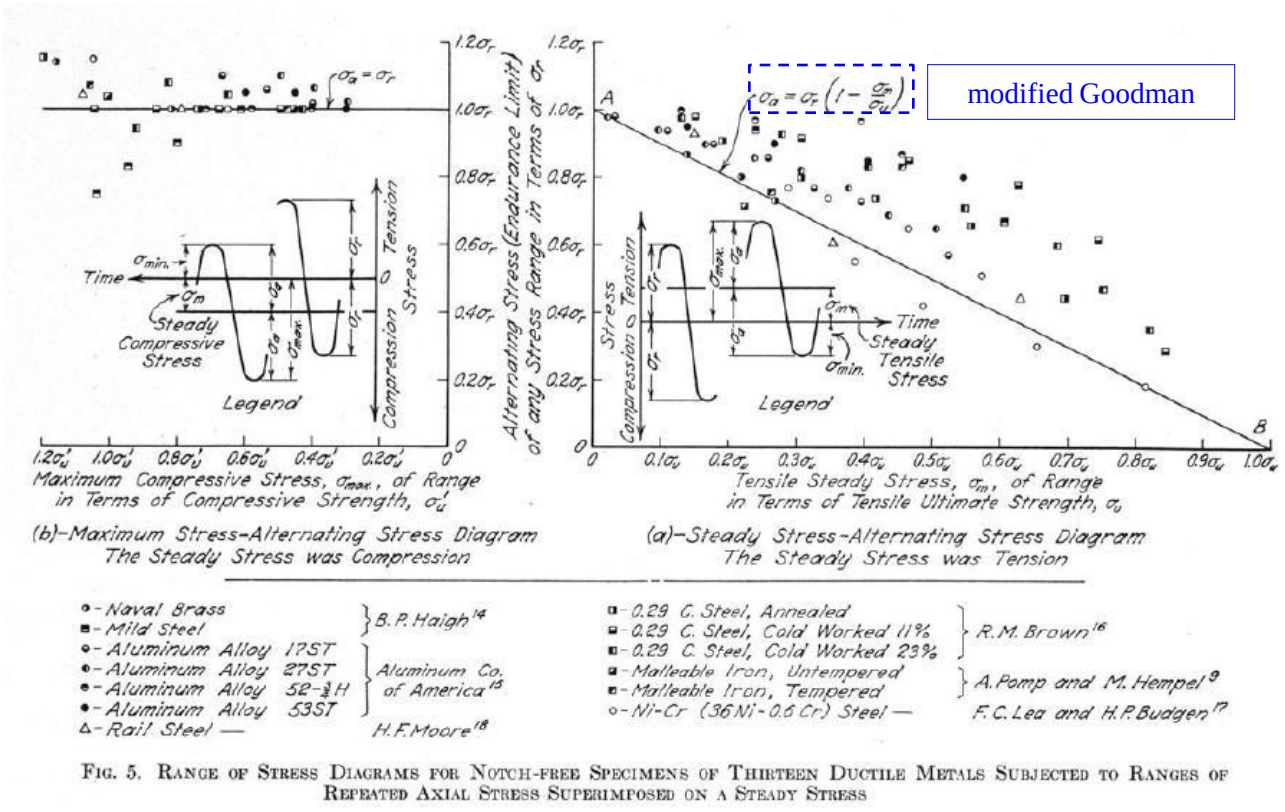

FIG. 5. RANGE OF STRESS DIAGRAMS FOR NOTCH-FREE SPECIMENS OF THIRTEEN DUCTILE METALS SUBJECTED TO RANGES OF REPEATED AXIAL STRESS SUPERIMPOSED ON A STEADY STRESS

Ref.: James O. Smith, **Univ. of Illinois Bulletin -The Effect of Range of Stress on the Fatigue Strength of Metals**, Vol. XXXIX, Feb. 17, 1942, No. 26, pg. 14, 20.

Mean Stress Empirical Relationships

The generation of S-N master diagrams is very expensive and time consuming. Empirical relationships that define the infinite life boundary afford a reasonable preliminary design option.

These methods result in various curves that connect the alternating stress (σ_a) and mean stresses (σ_m) to the endurance limit (S_e) and either the material yield (S_y), ultimate (S_u), or true fracture stress (σ_f).

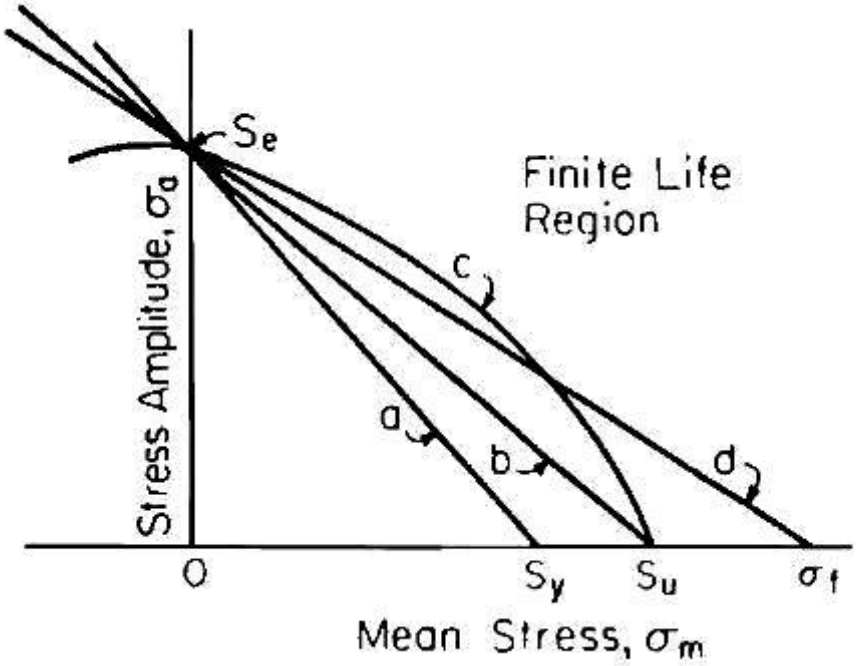

Soderberg (USA, 1930): $\frac{\sigma_a}{S_e} + \frac{\sigma_m}{S_y} = 1$

Goodman (England, 1899): $\frac{\sigma_a}{S_e} + \frac{\sigma_m}{S_u} = 1$

Gerber (Germany, 1874): $\frac{\sigma_a}{S_e} + \left(\frac{\sigma_m}{S_u}\right)^2 = 1$

Morrow (USA, 1960s): $\frac{\sigma_a}{S_e} + \frac{\sigma_m}{\sigma_f} = 1$

Figure 1.9 Comparison of mean stress equations (a. Soderberg, b. Goodman, c. Gerber, d. Morrow).

Ref.: Bannantine, J., Comer, J., Handrock, J., **Fundamentals of Metal Fatigue**, Prentice-Hall, 1990, pp. 6-7.

Mean Stress Constant Amplitude Service Life Example

***Note*: analytical result is dependent upon potential endurance limit variations/reductions & material data scatter (scatter factor).**

A component undergoes a cyclic stress with a maximum value of 110 ksi and a minimum value of 10 ksi. The component is made from a steel with an ultimate strength, S_u, of 150 ksi, an endurance limit, S_e, of 60 ksi, and a fully reversed stress at 1000 cycles, S_{1000}, of 110 ksi. Using the Goodman relationship, determine the life of the component.

Solution Determine the stress amplitude and mean stress.

$$\sigma_a = \frac{\sigma_{max} - \sigma_{min}}{2} = \frac{110 - 10}{2} = 50 \text{ ksi}$$

$$\sigma_m = \frac{\sigma_{max} + \sigma_{min}}{2} = \frac{110 + 10}{2} = 60 \text{ ksi}$$

Generate a Haigh diagram with constant life lines at 10^6 and 10^3 cycles. These lines are constructed by connecting the endurance limit, S_e, and S_{1000} values on the alternating stress axis to the ultimate strength, S_u, on the mean stress axis (see Fig. E1.1).

When the stress conditions for the component (σ_a = 50 ksi, σ_m = 60 ksi) are plotted on the Haigh diagram, the point falls between the 10^3 and 10^6 life lines. This indicates that the component will have a finite life, but the life is greater than 1000 cycles. Next, a line is drawn through the point representing the stress conditions and the ultimate strength, S_u, on the mean stress axis. This represents a constant life line at a life equal to the life of the component. This line intersects the fully reversed alternating stress axis at a value of 83 ksi. Note that this value could also be obtained by solving a modification of Eq. (1.9):

$$\frac{\sigma_a}{S_n} + \frac{\sigma_m}{S_u} = 1$$

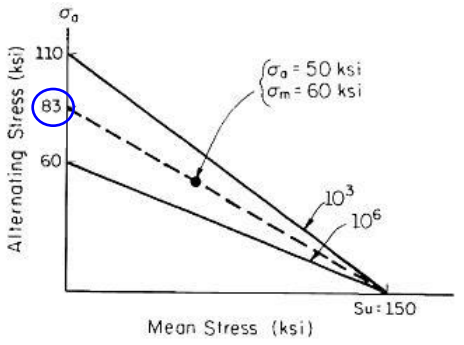

Figure E1.1 Haigh diagram.

where S_n is the fully reversed stress level corresponding to the same life as that obtained with the stress conditions σ_a and σ_m. For this problem,

$$\frac{50}{S_n} + \frac{60}{150} = 1$$

$$S_n = 83 \text{ ksi}$$

The value for S_n can now be entered on the S–N diagram (Fig. E1.2) to determine the life of the component, N_f. (Recall that the S–N diagram represents fully reversed loading). When a value of 83 ksi is entered on the S–N diagram for the material used for the component, the resulting life to failure, N_f, is 2.4×10^4 cycles.

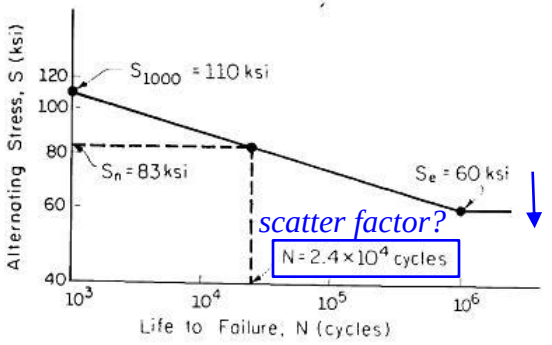

Figure E1.2 S–N diagram.

Ref.: Bannantine, J., Comer, J., Handrock, J., **Fundamentals of Metal Fatigue**, Prentice-Hall, 1990, pp. 8-9.

Palmgren-Miner Linear Damage Rule

In 1924 Palmgren uses linear damage accumulation to define the cycle life of bearings.
In 1945 Miner applies the Palmgren linear damage model to aircraft fatigue.

The shortcomings of assuming linear damage accumulation are well known (low-to-high or high-to-low loading sequences $\Sigma n_i/N_{fi} \neq 1$) but is still commonly incorporated due to ease of use and overall accuracy with respect to other models.

$$\sum \frac{n_i}{N_{fi}} = \frac{n_1}{N_{f1}} + \frac{n_2}{N_{f2}} + \ldots = 1$$

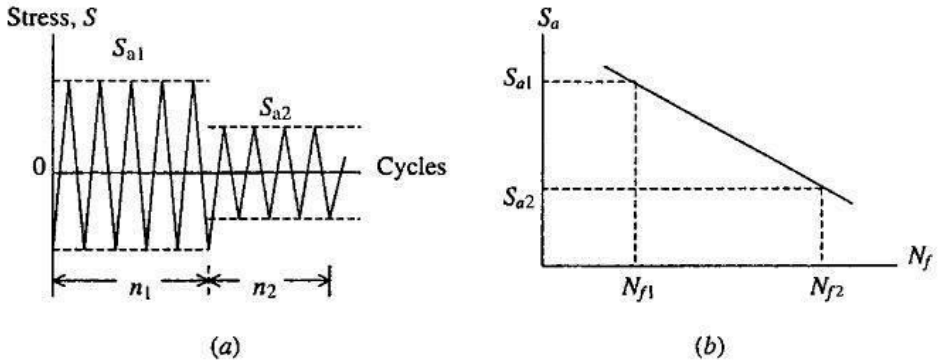

Figure 9.3 Constant amplitude stress blocks and S–N curve. (a) Constant amplitude stress blocks. (b) S–N curve.

$$D = \Sigma(n_i/N_{fi})^{\alpha i},$$

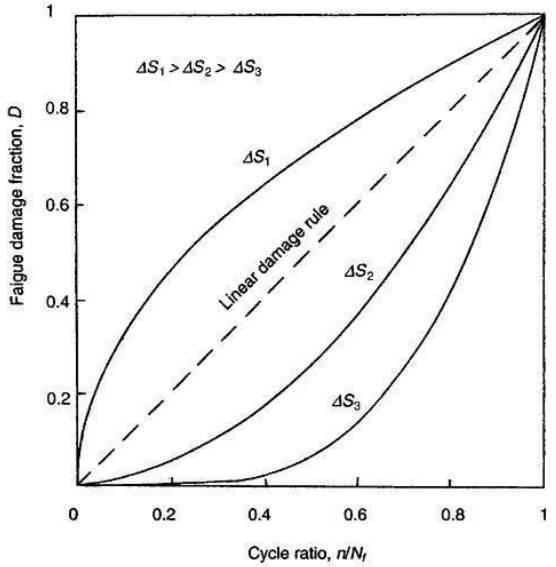

Figure 9.4 Fatigue damage fraction versus cycle ratio.

Ref.: R. I. Stephens, A. Fatemi, R. R. Stephens, H. Fuchs, "**Metal Fatigue in Engineering, 2nd ed.,"** John Wiley & Sons**,** 2000, pp. 275-276**.**

S-N Fatigue Endurance Limit

S-N Endurance Limit

Alloys that demonstrate a fatigue endurance limit (cyclic stress levels below which fatigue damage is assumed to not occur) and the mechanisms that can remove or eliminate the endurance limit are provided below.

S–N test data are usually presented on a log–log plot, with the actual S–N line representing the mean of the data. Certain materials, primarily body-centered cubic (BCC) steels, have an endurance or fatigue limit, S_e, which is a stress level below which the material has an "infinite" life (see Fig. 1.1). For engineering purposes, this "infinite" life is usually considered to be 1 million cycles. The endurance limit is due to interstitial elements, such as carbon or nitrogen in iron, which pin dislocations. This prevents the slip mechanism that leads to the formation of microcracks. Care must be taken when using the endurance limit since it can disappear due to:

1. Periodic overloads (which unpin dislocations)
2. Corrosive environments (due to fatigue corrosion interaction)
3. High temperatures (which mobilize dislocations)

Complex assemblies with relative movement that results in localized wear which degrades the initial surface condition relative to that which defined the endurance limit; e.g., bolted joints.

Ref.: Bannantine, J., Comer, J., Handrock, J., **Fundamentals of Metal Fatigue**, Prentice-Hall, 1990, pp. 2.

S-N Endurance Limit ; (cont)

A demonstration of periodic overloads removing the S-N fatigue endurance limit is provided below. Most structural applications deviate from the laboratory defined constant amplitude loading.

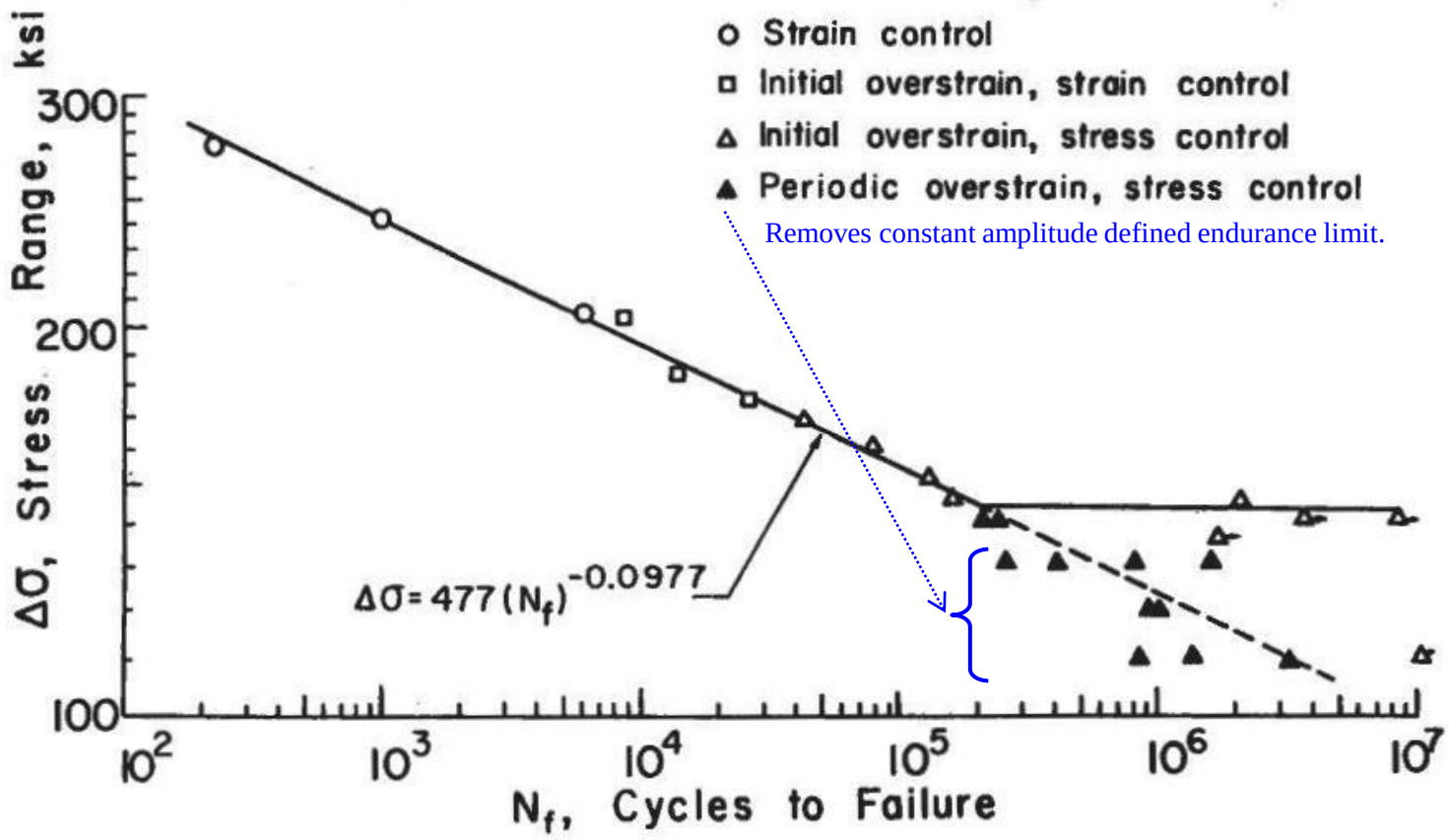

Fig. 19 Stress versus Life for SAE 4340 Steel (14)

Ref.: JoDean Morrow, J.F. Martin, N.E. Dowling, **Local Stress-Strain Approach to Cumulative Fatigue Damage Analysis**, UILU-ENG 74 6001, T.&A.M. Report No. 379, 1974, pg 51.

S-N Endurance Limit – Gigacycle Fatigue ; (cont)

Constant amplitude fatigue testing at ultra high cycles (gigacycles ; 10^9) demonstrates finite life at cycle counts beyond 10^6. The fatigue damage accumulation also shifts from surface to interior initiations.

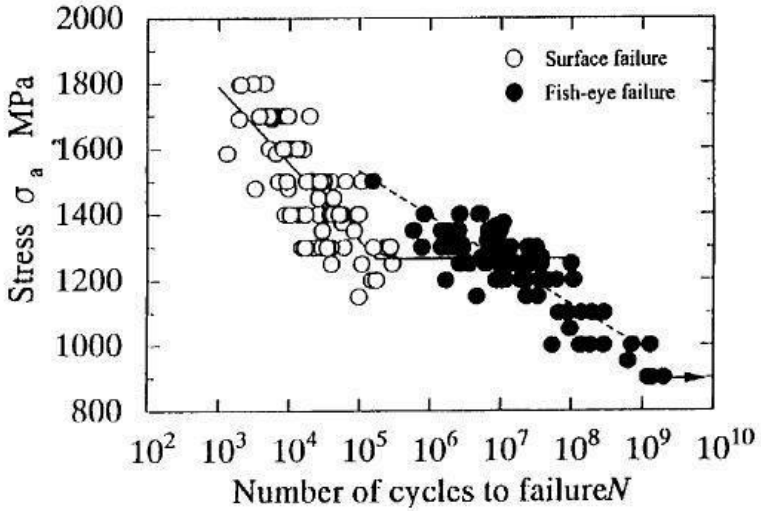

Figure 4.27 *S-N* curve of SUJ2 bearing steel ($R = -1$) r bending test (Sakai, 1999).

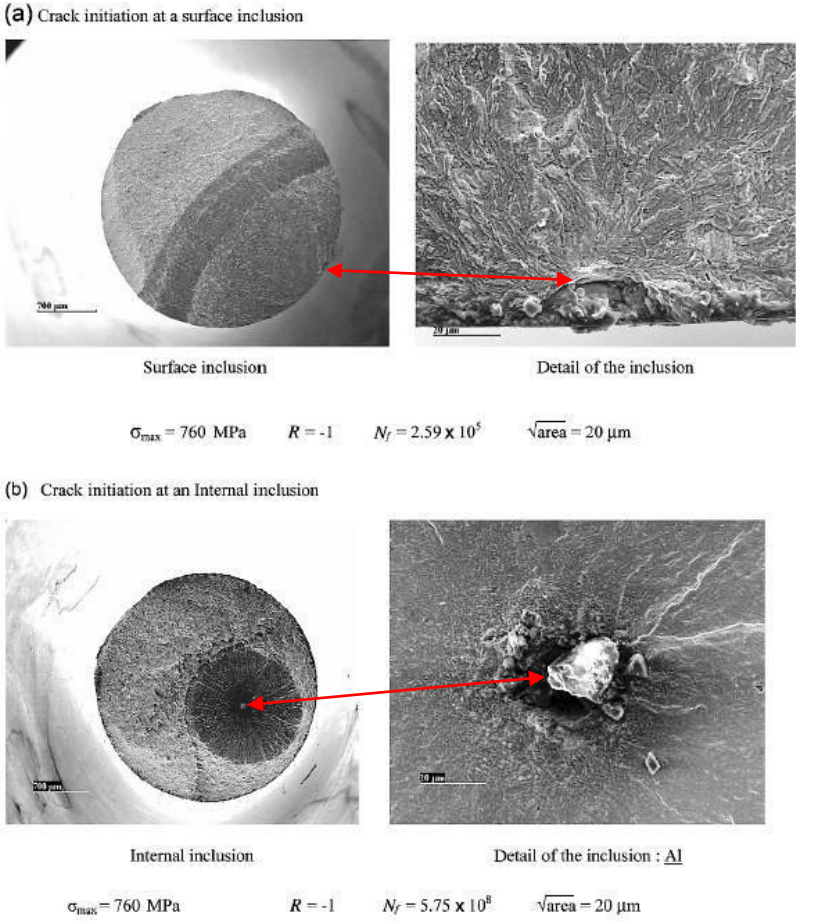

Figure 7.18 Surface-subsurface transition in crack initiation location in 4240 steel.

Ref.: C. Bathias, P.C. Paris, **Gigacycle Fatigue in Mechanical Practice**, Marcel Dekker, 2205.

S-N Fatigue Scatter

S-N Material Data Scatter

S-N data sets typical include only a few data points at various stress levels. The fatigue crack nucleation and initiation process constitutes the majority of the fatigue life and is highly dependent upon surface finish quality and microstructure. From a deterministic perspective a knockdown factor of 4 applied to the median of the S-N data set is assumed to define the lower bound for a complete S-N data set.

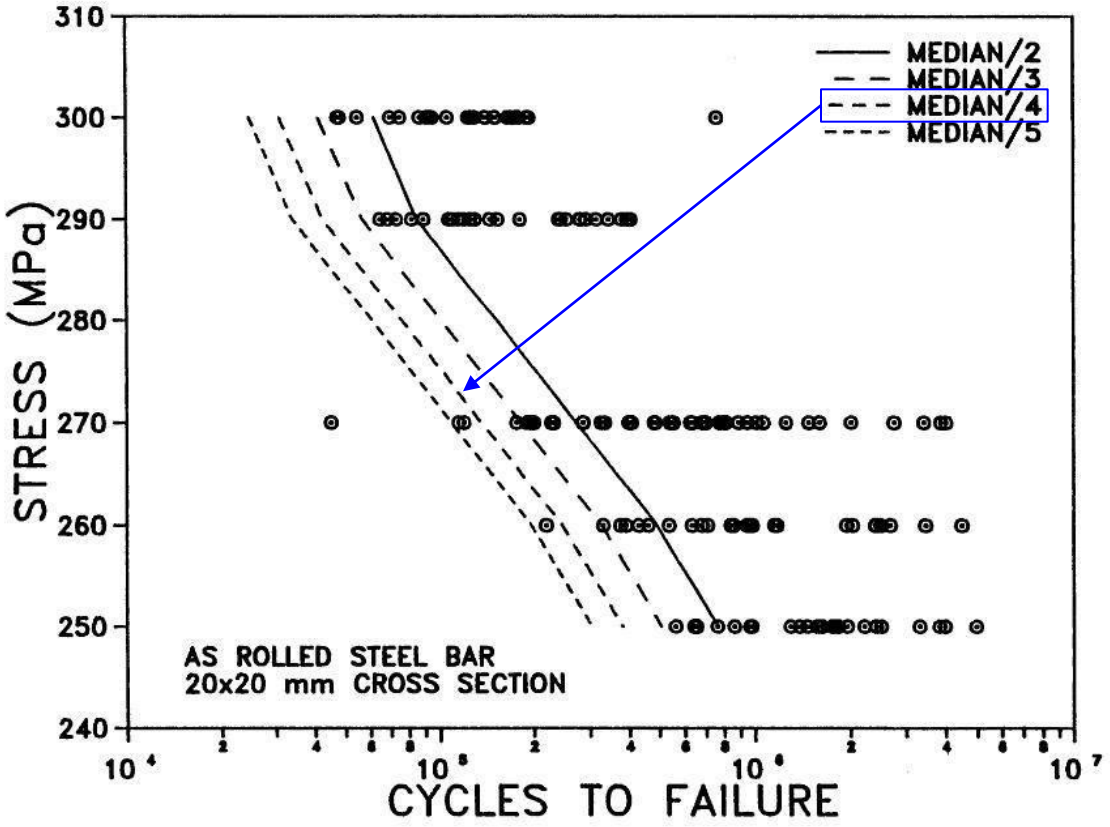

Figure 2 Constant Amplitude Cycles to Failure of Rolled Steel Bars

Ref.: A.P. Berens, **Fatigue Life Scatter Factors in Aircraft Applications**, UDR-TR-92-138, 1992.

S-N Material Data Scatter ; (cont)

The scatter factor of 4 is only applicable to the linear region of the S-N curve – it not applicable within the asymptotic regions of the data curve (endurance limit and material allowable). This result is confirmed in the results below wherein the variance of the S-N data set is no longer constant and increasing beyond 10^5 cycles.

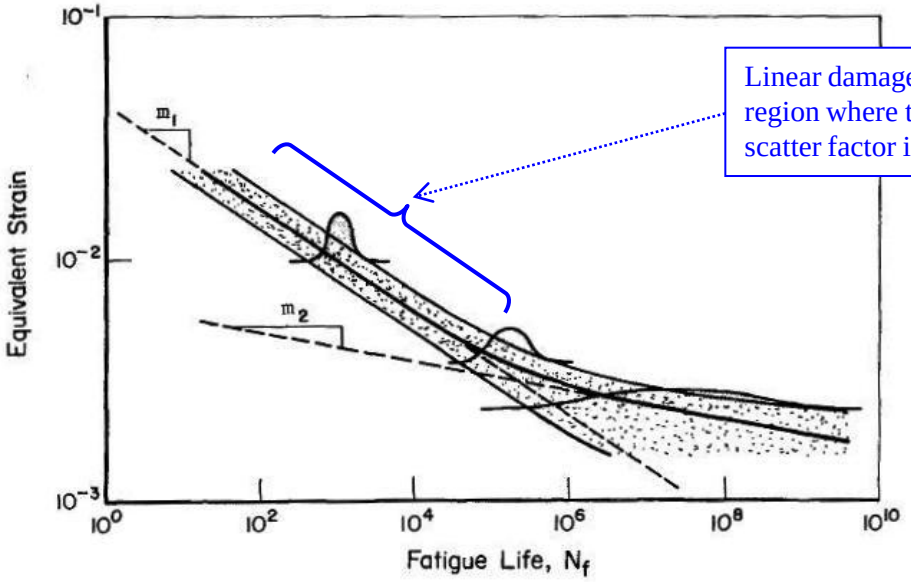

Figure 5. – Schematic illustration of typical fatigue data trends in the region from 10^2 to 10^8 cycles to failure.

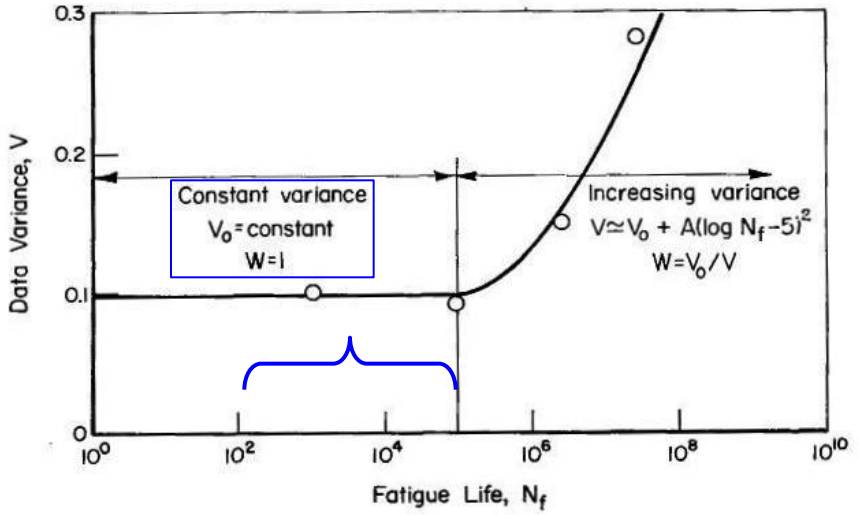

Figure 6. – Illustration of increasing variance for $N_f > 10^5$ cycles and an approximate function describing these trends.

Ref.: R.C. Rice, K.B. Daview, C.E. Jaske, and C.E. Feddersen, **Consolidation of Fatigue and Fatigue Crack Propagation Data for Design Use,** NASA-CR-2586, 1975, pp. 24-25.

S-N Material Data Scatter ; (cont)

The S-N fatigue asymptotic regions wherein the traditional scatter factor on life does not assure the desired level of structural integrity assurance is illustrated below.

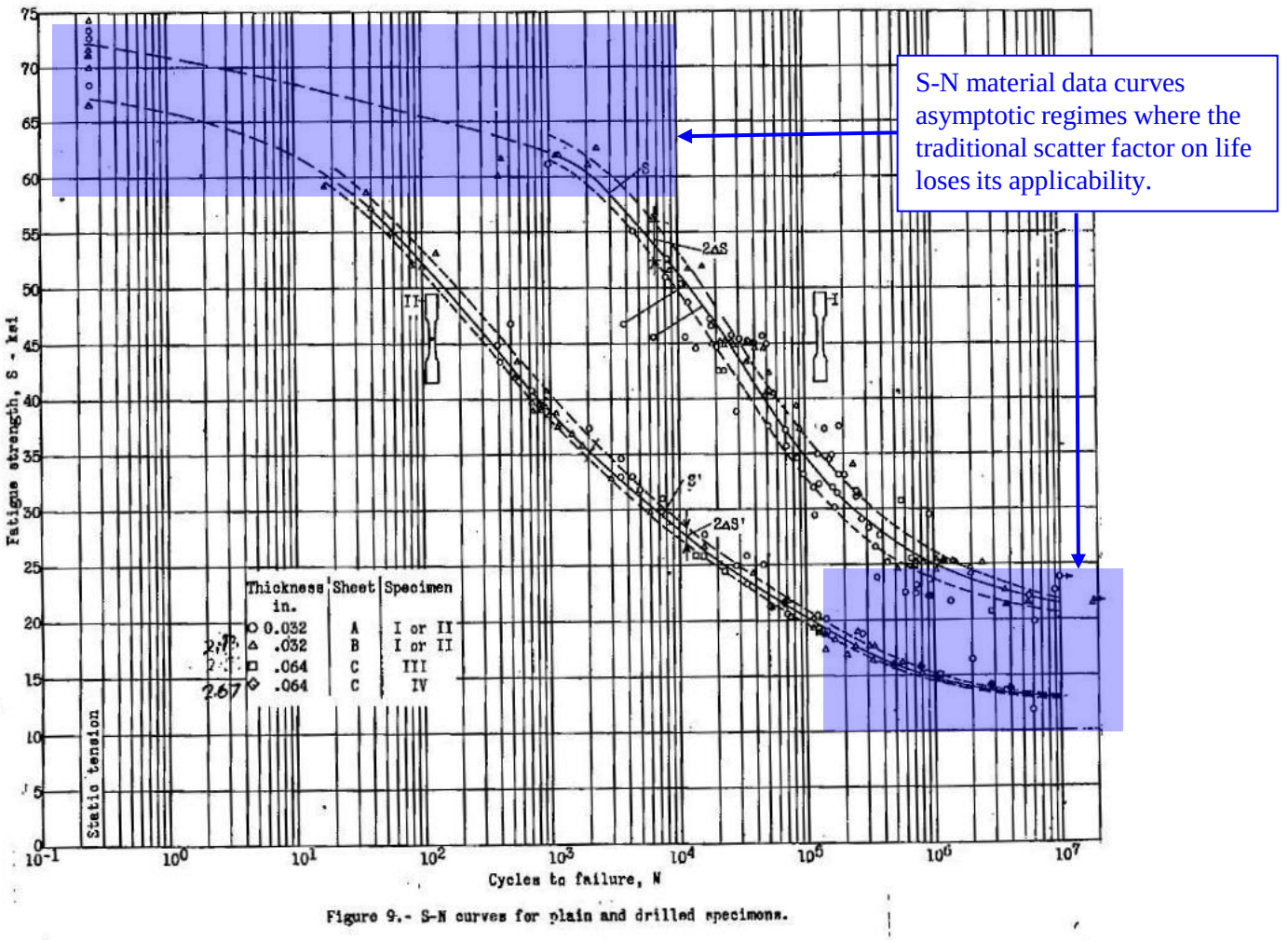

Figure 9.- S-N curves for plain and drilled specimens.

Ref.:W.C. Brueggeman, M. Mayer, Jr., and W.H. Smith, **Axial Fatigue Tests at Zero Mean Stress of 24S-T Aluminum-Alloy Sheet With and Without a Circular Hole**, NACA TN 995 1944.

S-N Scatter (cont.) - Full Scale Test Results

"*It can be seen from this figure that all of the full-scale data presented lie within a comparatively narrow scatter band, considering the fact that the data includes different types of airplanes and components with many types of stress raisers. Full-scale fatigue data from other airplanes have been found to fall within the scatter of the data that are presented*."

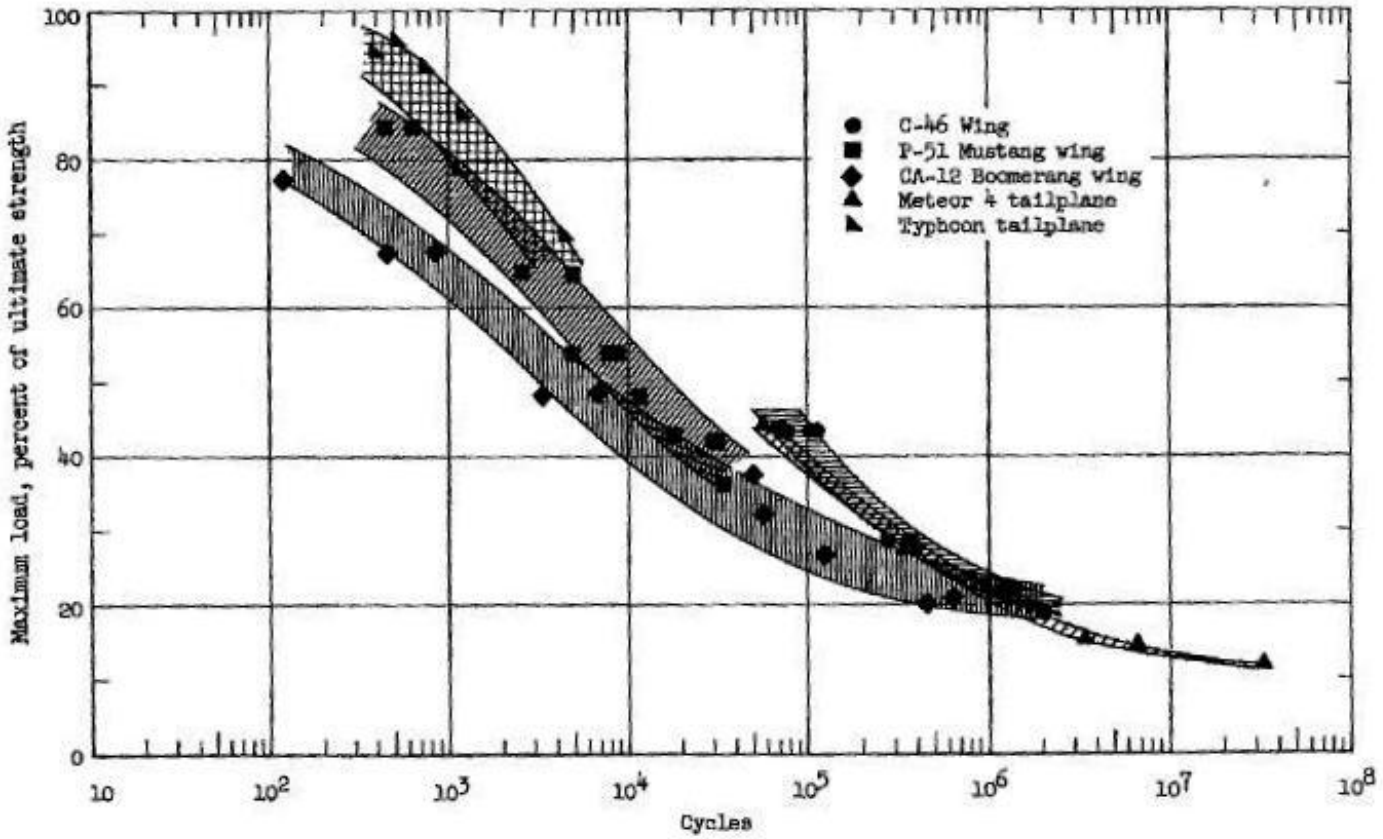

Figure 13.- Load-lifetime diagrams for several aircraft structures.

Ref.: J.J. McGuigan, Jr. D.F. Bryan, and R.E. Whaley, **Fatigue Investigation of Full-Scale Transport Airplane Wings**, NACA TN 3190, 1954, pg. 10, 41.

Torsion Fatigue

Modes of Crack Surface Displacements

The 3 basics modes of loading and displacements associated with cracked elastic bodies is presented below. The superposition of these 3 displacement modes is typically sufficient to describe most crack tip deformation/stress fields.

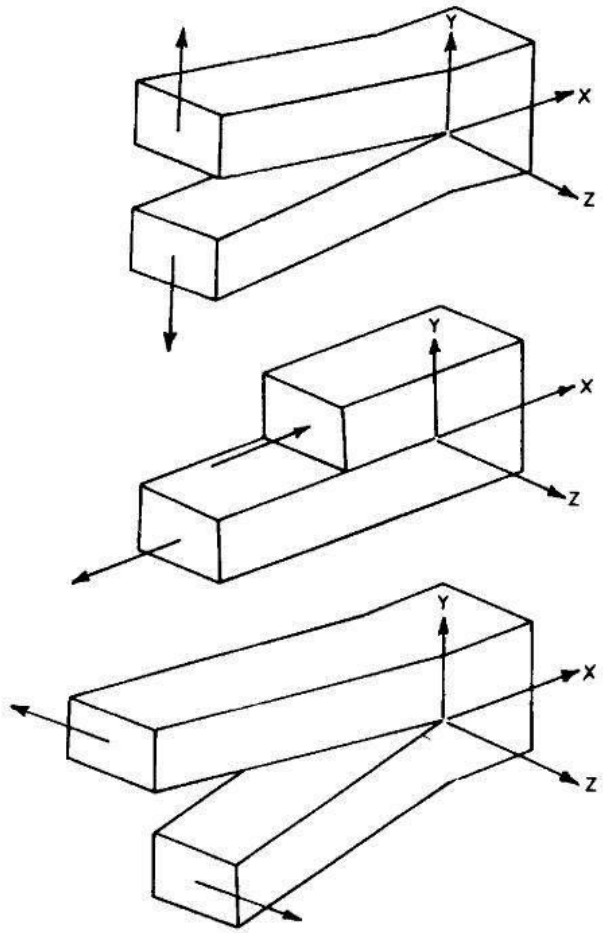

Mode I – tensile opening mode ; the crack surfaces are displaced away from each other (symmetric with respect to the x-y and x-z planes.

Mode II – in-plane (edge) sliding of the crack faces relative to each other ; symmetric with respect to the x-y plane and skew symmetric with respect to the x-z plane.

Mode III – lateral displacement of the crack faces (tearing) ; skew symmetric with respect to the x-y and x-z planes.

Ref.: H. Tada, P. Paris, & G. Irwin, **The Stress Analysis of Cracks, 2nd ed.**, Del Research Inc, 1985, pg. 1.2.

Torsion Induced Stress Fields

Torsion loading (round cross section) will result in maximum shear stresses on the longitudinal and transverse planes with axial stresses on 45° planes.

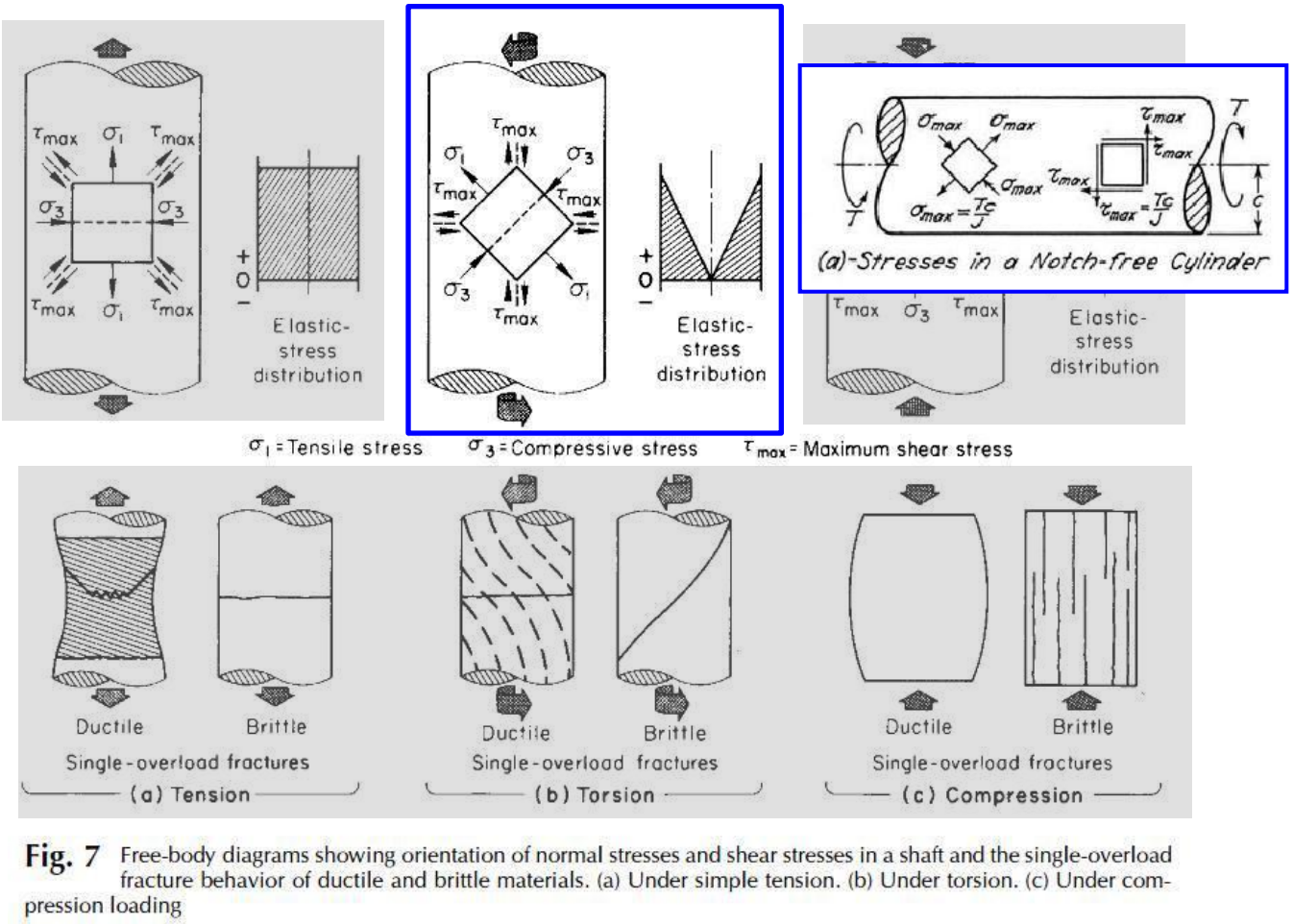

Fig. 7 Free-body diagrams showing orientation of normal stresses and shear stresses in a shaft and the single-overload fracture behavior of ductile and brittle materials. (a) Under simple tension. (b) Under torsion. (c) Under compression loading

Ref.: **ASM Handbook, Vol. 11 Failure Analysis Prevention**, J.D. Landes, W.T. Becker, R.S. Shipley, J. Raphael, ***Stress Analysis and Fracture Mechanics***, ASM International, 2002, pg. 467.

Torsion Induced Fatigue Cracking Pattern/Modes

Torsion loading (round cross section) fatigue cracking pattern is a function of the applied shear stress magnitude.

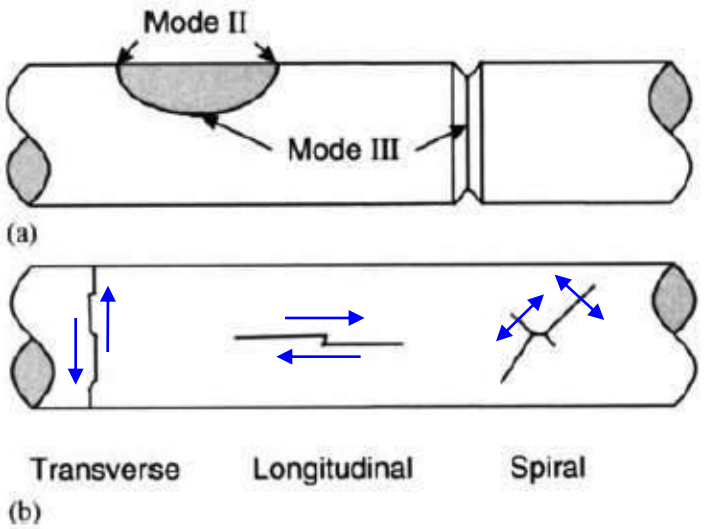

Figure 7 (a) Crack stress intensity modes and (b) failure patterns for shafts in torsion.

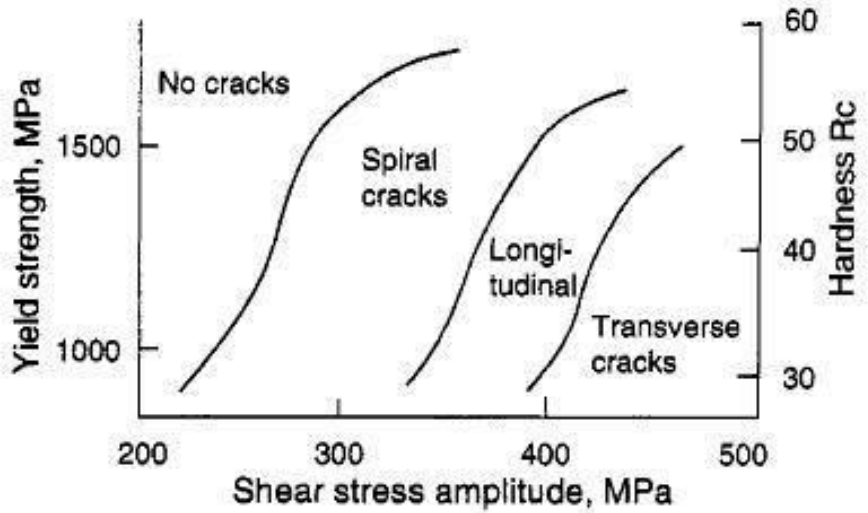

Figure 8 Macroscopic fracture mechanism map for torsion (after Hu *et al.*, 1992).

Ref.: G.B. Marquis, D.F. Socie, "**Multiaxial Fatigue**", Chapter 4.09, *Volume 1, Examples and Case Studies*, R. O. Ritchie and Y. Murakami, volume editors, part of the 10-volume set, ***Comprehensive Structural Integrity***, B. Karihaloo, R. O. Ritchie, and I. Milne, overall editors, Elsevier Science Ltd. Oxford, England, 2003.

Torsion Fatigue Failure Cracking Pattern Examples

Spiral reversed torsion fatigue crack

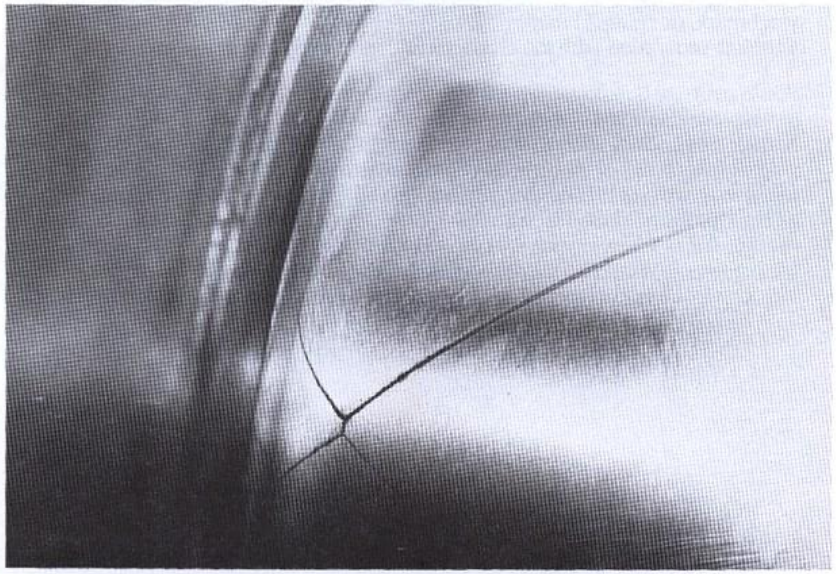

Fig. 29 Characteristic X-shaped crack pattern in a 1045 steel crankshaft after testing in reversed torsional fatigue in a special machine, not in an engine. In this case, the original crack was in the transverse shear plane, not in the longitudinal shear plane as in Fig. 28.

Transverse reversed torsion fatigue crack

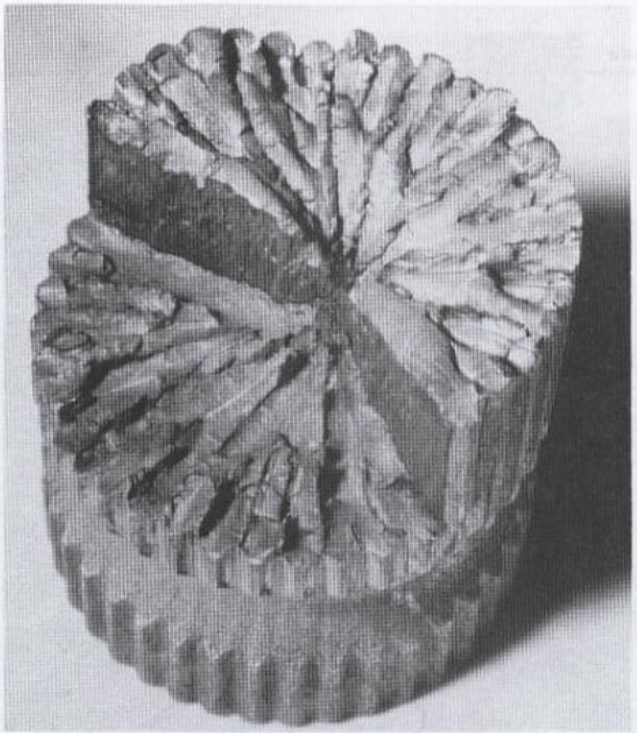

Fig. 31 A "starry" spline fracture similar to that in Fig. 30 due to reversed torsional fatigue on a 1½ in. diam spline. Torsional fatigue has caused many of the surrounded segments to fall out of the shaft. Note that the longitudinal cracks penetrated nearly to the center of the shaft. This part is made from low-carbon alloy steel with a hardness of 24 HRC in the shaft area.

Ref.: Donald J. Wulpi, **Understanding How Components Fail, 2nd edition**, ASM International 1999, pp. 158,160.

Torsion Fatigue Data

Smooth bar torsion fatigue data for various materials with constant cyclic stress amplitude does not demonstrate the same Goodman trend established for tensile (Mode I) fatigue data.

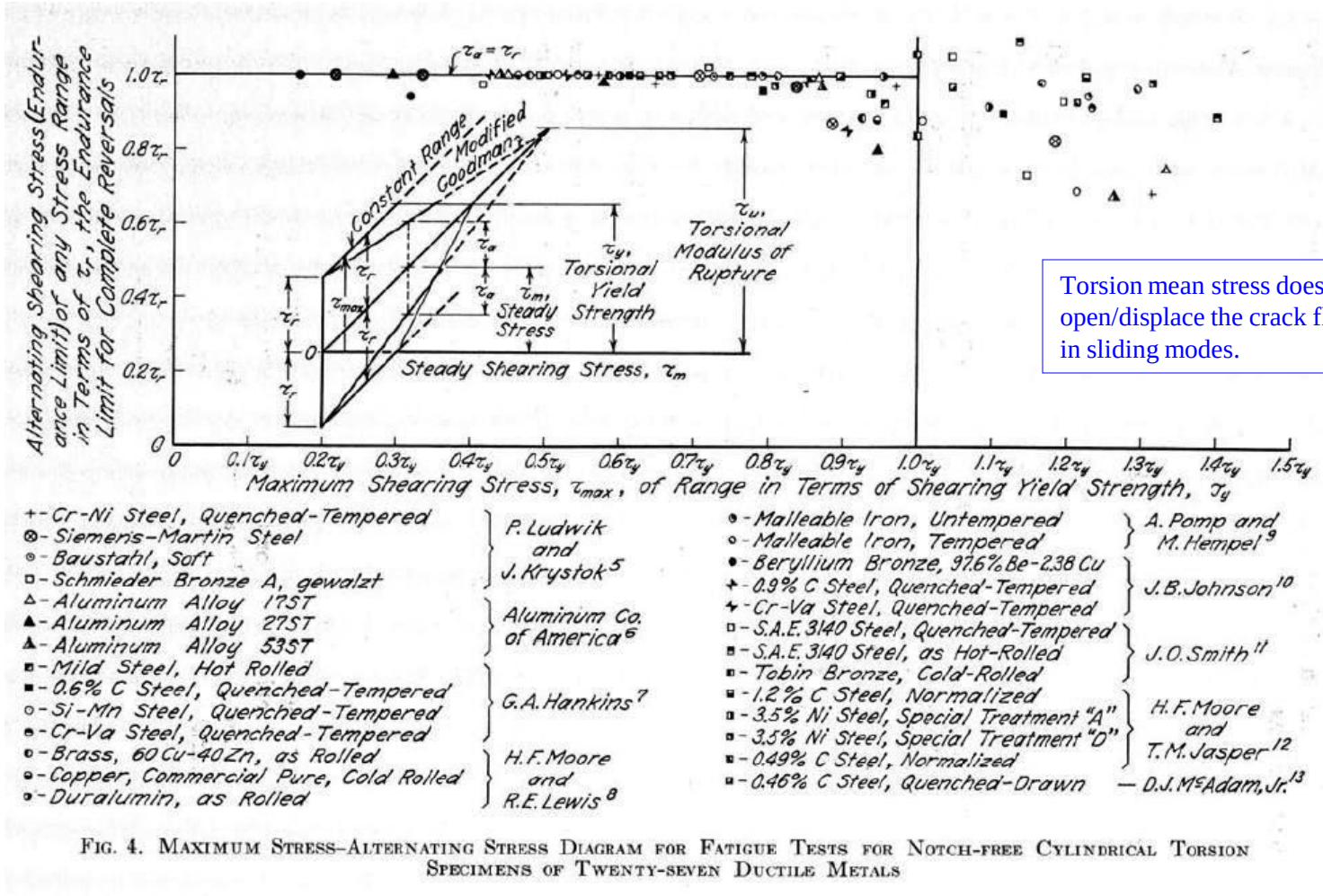

FIG. 4. MAXIMUM STRESS–ALTERNATING STRESS DIAGRAM FOR FATIGUE TESTS FOR NOTCH-FREE CYLINDRICAL TORSION SPECIMENS OF TWENTY-SEVEN DUCTILE METALS

Torsion mean stress does not open/displace the crack flanks in sliding modes.

Ref.: James O. Smith, **Univ. of Illinois Bulletin -The Effect of Range of Stress on the Fatigue Strength of Metals**, Vol. XXXIX, Feb. 17, 1942, No. 26, pg. 18.

Torsion Fatigue Data ; (cont.)

Notched bar torsion fatigue data for various materials with constant cyclic stress amplitude does demonstrate a similar Goodman trend established for tensile (Mode I) fatigue data.

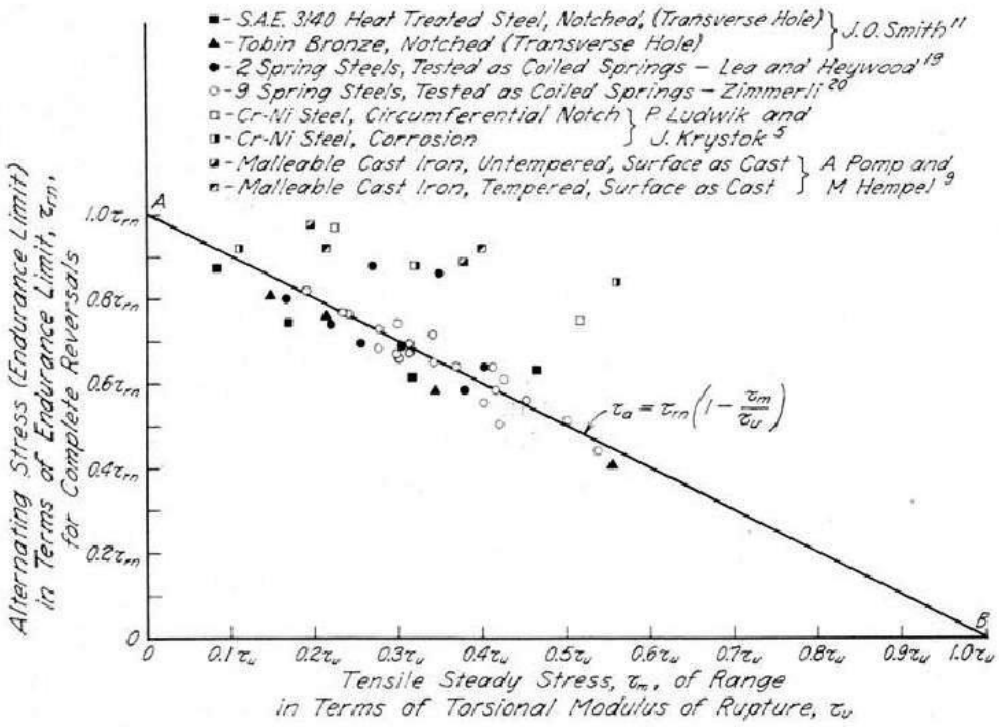

FIG. 6. STEADY STRESS–ALTERNATING STRESS DIAGRAM FOR TORSIONAL FATIGUE TESTS OF NOTCHED SPECIMENS OF SEVENTEEN DUCTILE METALS

Ref.: James O. Smith, **Univ. of Illinois Bulletin -The Effect of Range of Stress on the Fatigue Strength of Metals**, Vol. XXXIX, Feb. 17, 1942, No. 26, pg. 22.

For shafts having circumferential notches or shoulders, low torsional stress amplitudes will produce "factory-roof" type fracture surfaces such as the one shown on the right-hand side of Figure 9 for a 30 mm diameter shaft. These cracks grow locally by mode I and are irregularly shaped as the crack alternates between both maximum tension planes. Compare this fracture surface with that of bending. The irregular crack pattern results in a significant degree of interlocking which reduces the crack driving force. These mode III cracks do not grow as fast as mode I cracks. At higher torsional load amplitudes, relatively flat circumferential shear cracks develop at the root of the notch.

Ref.: G.B. Marquis, D.F. Socie, "**Multiaxial Fatigue**", Chapter 4.09, *Volume 1, Examples and Case Studies*, R. O. Ritchie and Y. Murakami, volume editors, part of the 10-volume set, ***Comprehensive Structural Integrity***, B. Karihaloo, R. O. Ritchie, and I. Milne, overall editors, Elsevier Science Ltd. Oxford, England, 2003.

Mechanics of Fatigue Damage Accumulation

Plastic Deformation in Metals

The elastic limit of a material defines the stress level below which the strains are reversible (on a global level – measurable on a macroscopic scale).

Plastic (irreversible) deformation occurs primarily by slip along crystallographic planes – the slip mechanism is dictated by local shear stresses and crystal defect orientations.

Defects and imperfections within the crystalline lattice create slip systems along specific planes and in specific directions along a plane. Dislocations (edge & screw) are line defects that exist in nearly all crystals.

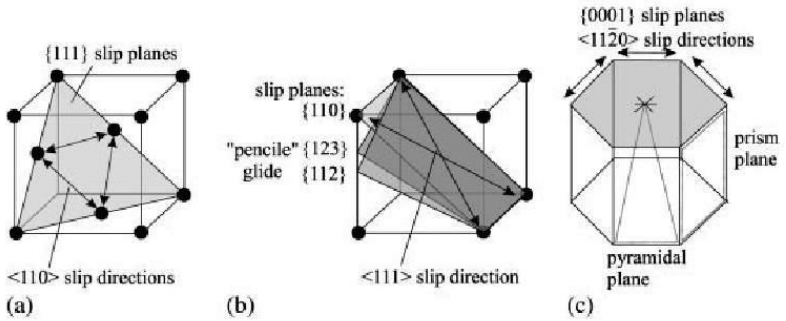

Fig. 4.14 Slip systems in (a) fcc, (b) bcc and (c) hexagonal crystal systems.

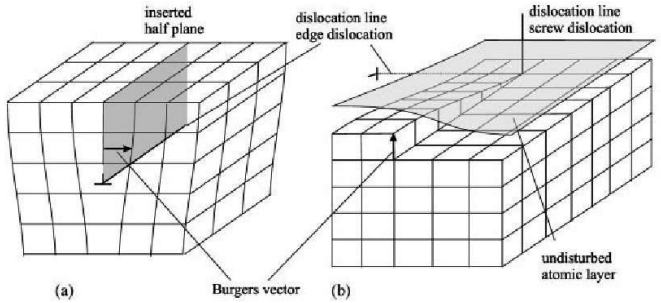

Fig. 4.5 Simplified representation of (a) an edge dislocation and (b) a screw dislocation, the latter in combination with an edge dislocation (see dashed line).

Ref.: U. Krupp, **Fatigue Crack Propagation in Metals and Alloys**, Wiley, 2007.

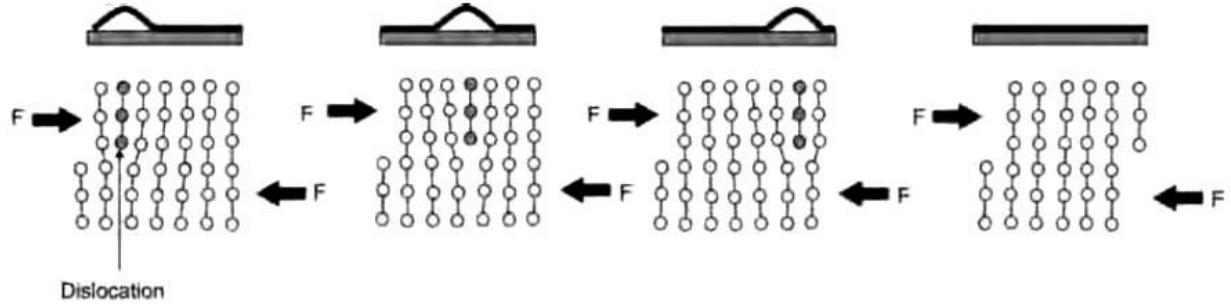

Fig 2.15 Line dislocation movement. The top illustrates the analogy of moving a rug with progression of a wrinkle. Source: Ref

Ref.: A.C. Reardon, **Metallurgy for the Non-Metallurgist - 2nd Ed.**, ASM International, 2011.

Plastic Deformation in Metals – Monotonic & Cyclic Loading

When the resolved shear stress exceeds the critical shear stress on the crystal slip plane local yielding will begin. The slip direction will remain unchanged unless barriers/constraints (e.g., adjacent grains, test grips) are encountered. Cyclic slip is not reversible (due to defect creation/annihilation) and this results is surface extrusions/intrusions along persistent slip bands on the surface.

montonic plastic strain

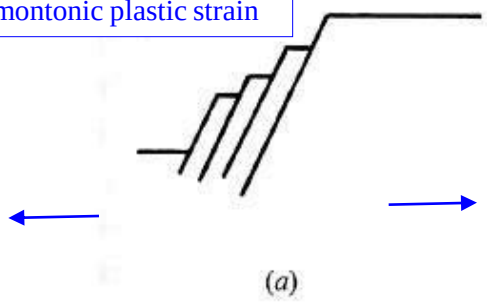

(a)

cyclic plastic strain

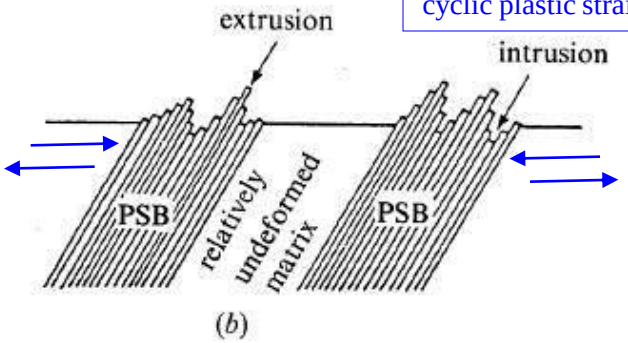

(b)

Ref.: V. Levitin, S. Loskutove, **Strained Metallic Surfaces**, Wiley-VCH, 2009, pg 187.

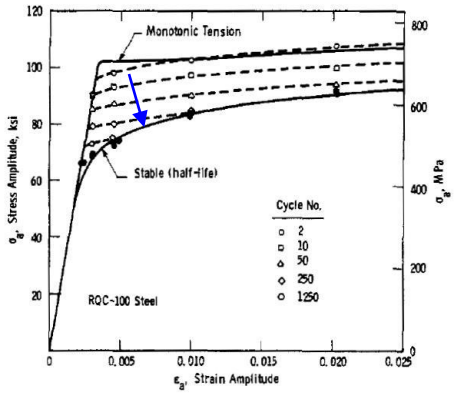

Figure 5 Cyclic and monotonic stress–strain curves for RQC-100 quenched and tempered low-alloy steel (reproduced from Dowling, 1978, with permission; © ASME).

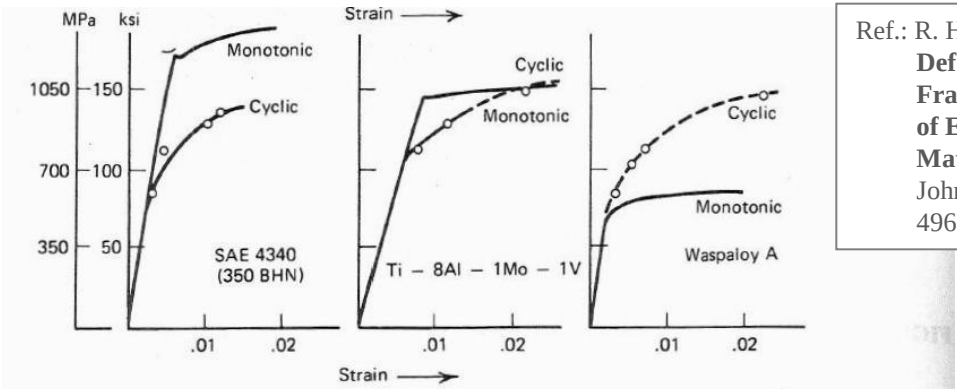

FIGURE 12.36 Monotonic and cyclic stress–strain curves for several engineering alloys.[55] (Reprinted by permission of the American Society for Testing and Materials from copyrighted work.)

Ref.: R. Hertzberg, **Deformation and Fracture Mechanics of Engineering Materials, 3rd Ed.**, John-Wiley, 1989, pg 496.

Fatigue Crack Nucleation (Surface)

The preferential nucleation of fatigue cracks at the surface is due to ease of plastic deformation at the free surface (as opposed to the interior where there is additional constraint). Fatigue cracks can also nucleate at singularities or discontinuities (e.g., inclusions, second phase particles, grain boundaries, etc.) on the surface or in the interior.

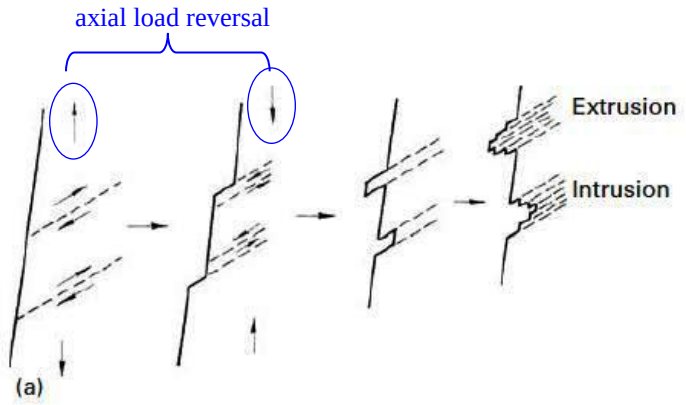

Fig. 14.13 (a) Fatigue crack nucleation at slip bands. (b) SEM of extrusions and intrusions in a copper sheet. (Courtesy of M. Judelwicz and B. Ilschner.)

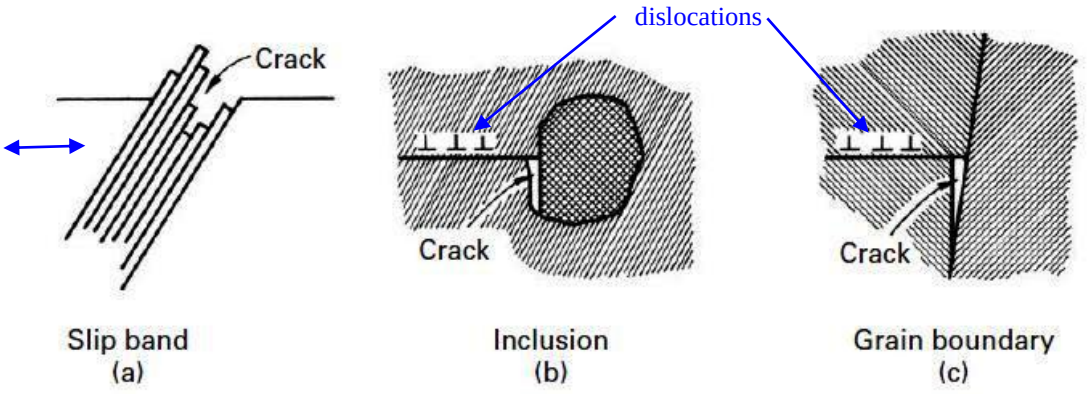

Fig. 14.14 Some mechanisms of fatigue crack nucleation. (After J. C. Grosskreutz, *Tech. Rep. AFML-TR-70–55* (Wright–Patterson AFB, OH: Air Force Materials Laboratory), 1970.)

Ref.: M.A. Meyers, K.K. Chawla, "**Mechanical Behavior of Materials,**" Cambridge University Press**,** 2009, pp. 725-729**.**

Micro Crack Initiation/Propagation (Surface)

Cyclic loading induced fatigue crack nucleation will result in multiple crack initiation sites within the stress concentration region of the component. The local microstructure and surface conditions strongly influence the resulting localized slip responses and subsequent coalescence into micro cracks..

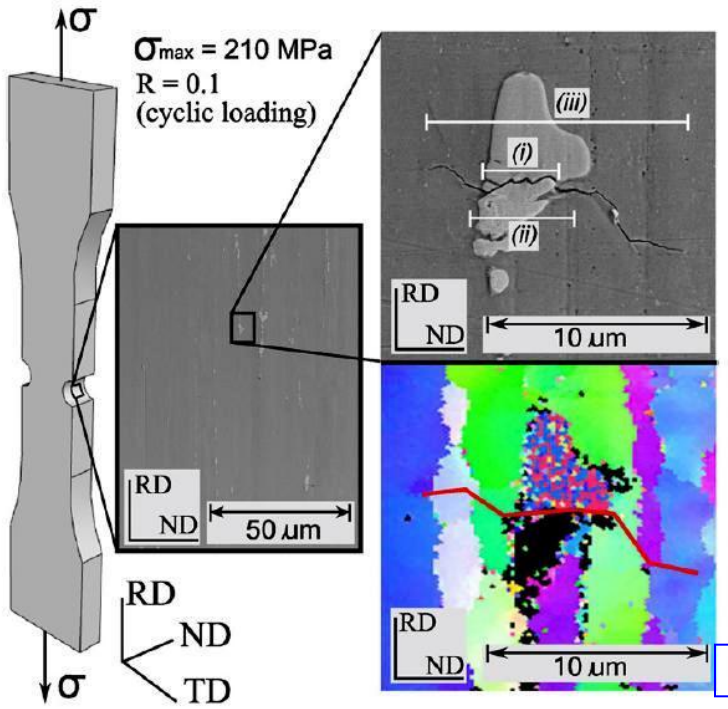

Figure 1. Double edge-notched specimen with cyclic loading applied in the RD (left). Observation window at notch root in which scanning electron microscopy was used to track the stages of MSFC throughout 3000 load cycles to track the MSFC phase (center). Cracked Al_7Cu_2Fe particle inclusion at 3000 load cycles, and corresponding grain orientations, in AA 7075-T651 that has undergone (i) incubation, (ii) nucleation and (iii) microstructurally small propagation (right).

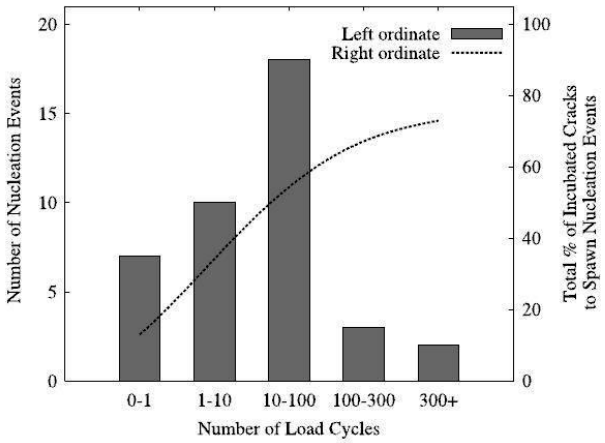

Figure 2. A histogram of the cycles at which nucleation events occurred for the AA 7075-T651 DEN specimen. Approximately 73% of the observed incubated cracks led to nucleated cracks into a surrounding grain.

10 μm = 0.000394 inches

MSFC – microstructurally small fatigue crack

Micro Crack Initiation/Propagation (Surface) – (cont.)

Another example of micro crack initiation and propagation is provided below.

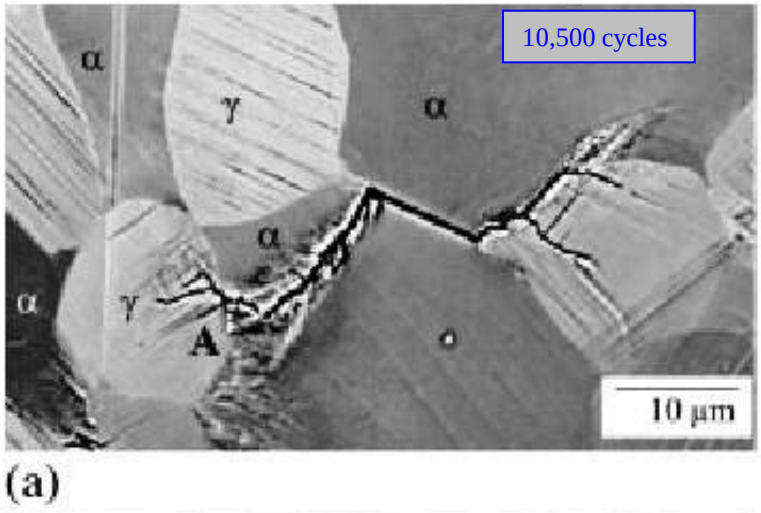

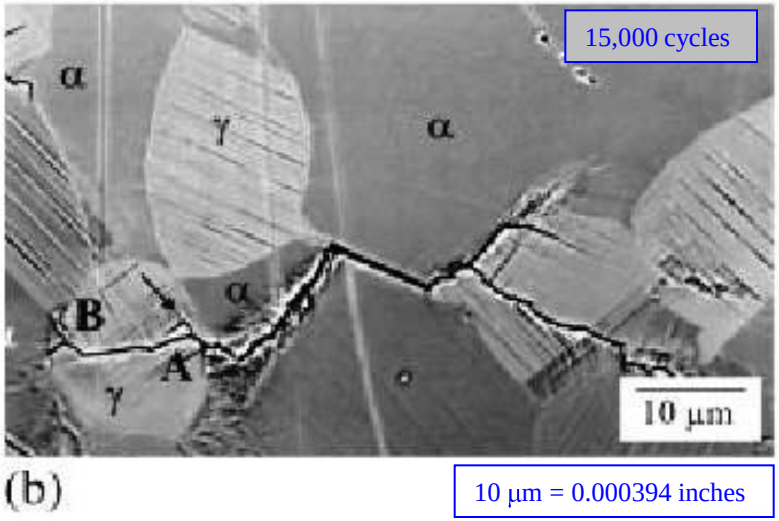

10 μm = 0.000394 inches

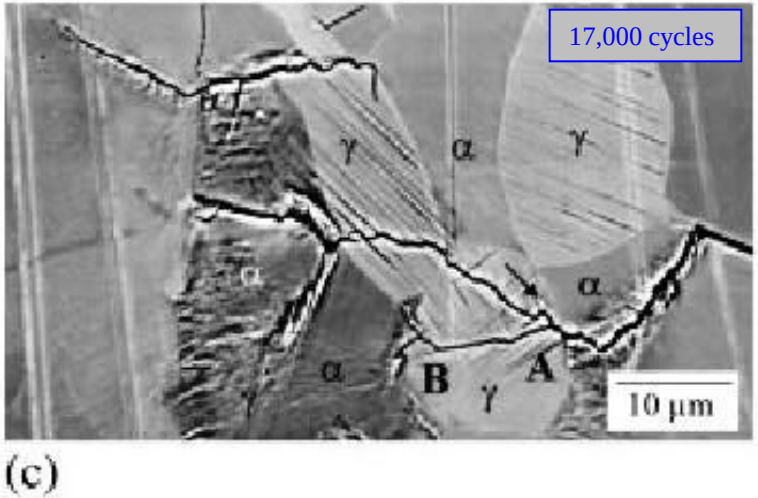

Fig. 6.15 Microcrack propagation in AISI F51 duplex steel during fatigue at $\Delta\sigma/2 = 550$ MPa (loading axis: ⇕) after (a) 10500 cycles, (b) 15000 cycles, (c) 17000 cycles. (d) Summary of the corresponding crack lengths vs. numbers of cycles data (for details see text).

Ref.: Ulrich Krupp, "**Fatigue Crack Propagation in Metals and Alloys,**" Wiley-VCH, 2007, pp. 151.

Crack Propagation Transition : Mode II (short crack) to Mode I (long crack)

The resolved shear stress (mode II) mechanism that dictates the surface crack initiation within slip bands is primarily responsible for the subsequent small crack initiation/propagation. As the micro crack growth extends over several grains the single slip mechanism transitions into a multiple slip response that results in mode I crack propagation response.

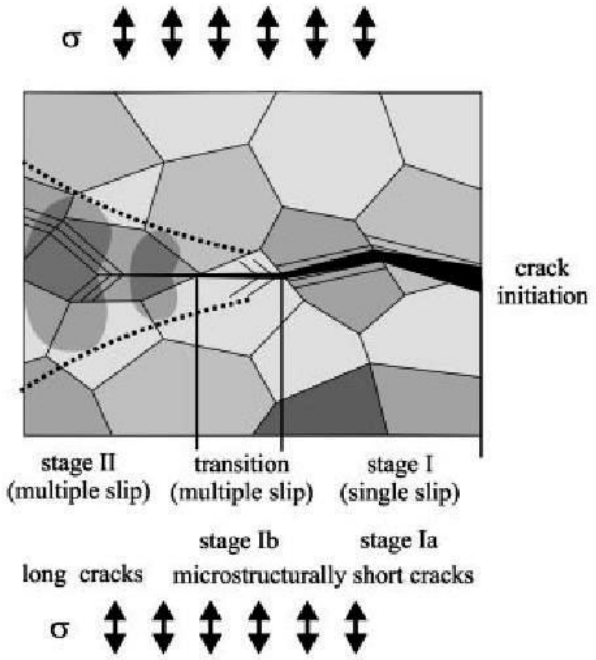

Fig. 6.33 Transition from stage I (stage Ia: shear-stress-controlled; stage Ib: normal-stress-controlled) to stage II crack propagation (normal-stress-controlled).

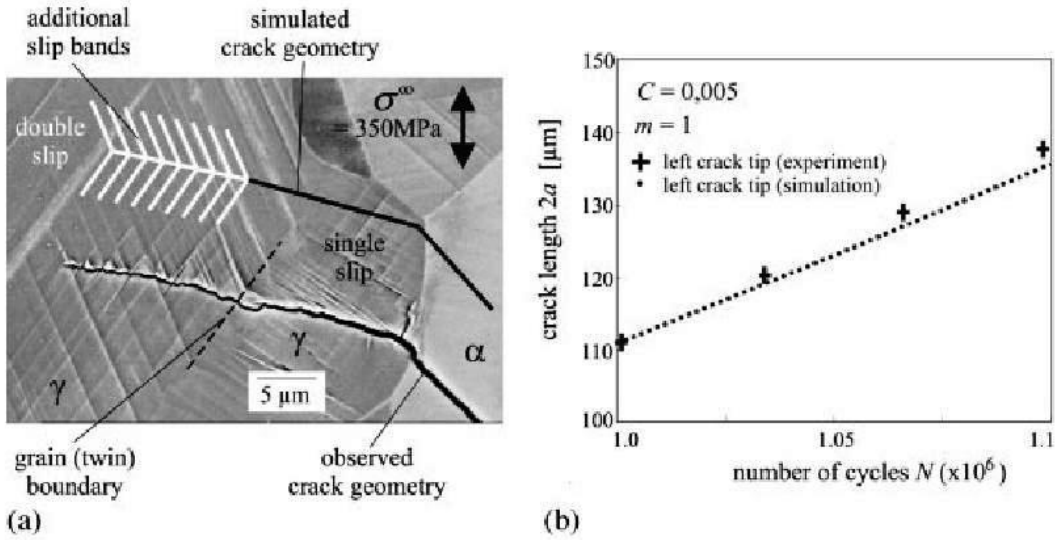

Fig. 7.22 Microcrack in AISI F51 8 duplex steel propagating by alternate operating slip systems: (a) scanning electron micrograph showing the crack path and activated slip bands; (b) comparison of the calculated and measured crack length vs. the number of cycles (after [334]).

Ref.: Ulrich Krupp, "**Fatigue Crack Propagation in Metals and Alloys,**" Wiley-VCH**,** 2007, pp. 172, 239**.**

Long Crack Propagation (Mode I) - Striations

The Mode I fatigue crack propagation occurs via dislocation movements along multiple slip planes in the vicinity of the crack tip. The irreversible nature of the slip response can result in the formation of microscopically visible steps on the fracture surface known as striations. Detectable striations are not always formed - dependent upon material, environment, and rate of crack propagation.

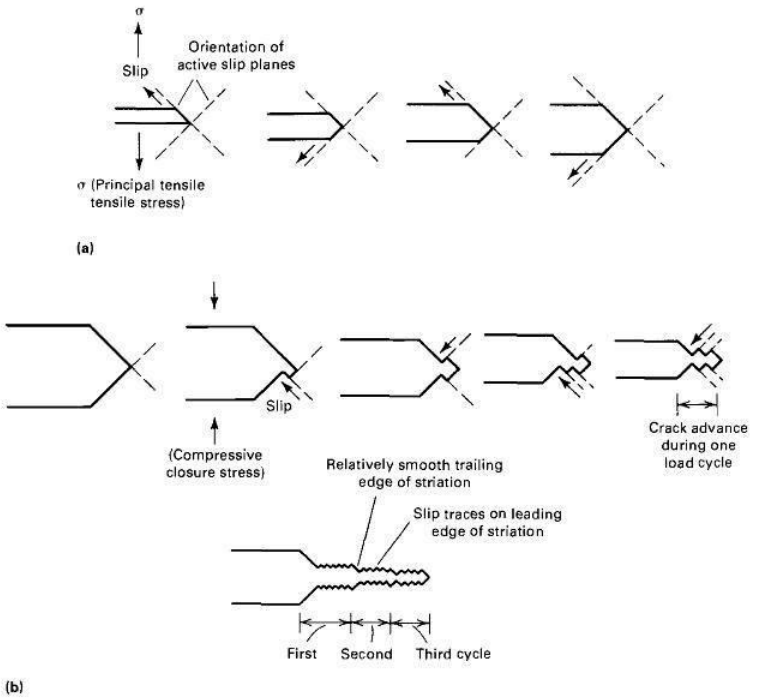

Fig. 23 Mechanism of fatigue crack propagation by alternate slip at the crack tip. Sketches are simplified to clarify the basic concepts. (a) Crack opening and crack tip blunting by slip on alternate slip planes with increasing tensile stress. (b) Crack closure and crack tip resharpening by partial slip reversal on alternate slip planes with increasing compressive stress

Ref.: V. Kerlins, **ASM Handbook Vol. 12 : Fractography**, 1987, pg 21.

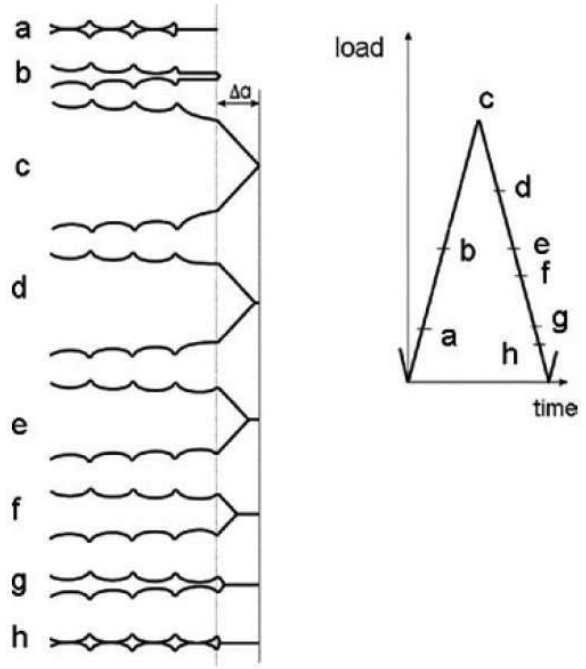

Fig. 5 Schematic representation of the crack tip deformation and propagation model obtained from the different 3D shapes of the crack tip during cyclic loading.

Ref.: Pippan, Zelger, Gach, Bichler, Weinhandl, **On the mechanism of fatigue crack propagation in ductile metallic materials**, Fatigue & Fracture of Engineering Materials & Structures, 34**,** 2010, pp. 1-16.

Long Crack Propagation (Mode I) – Striations (cont.)

Within a failure analysis investigation striations can be used to physically quantify aspects of the fatigue crack propagation which in turn can be used to calculate the corresponding structural response states (loading type, loading magnitude, number of cycles, etc.).

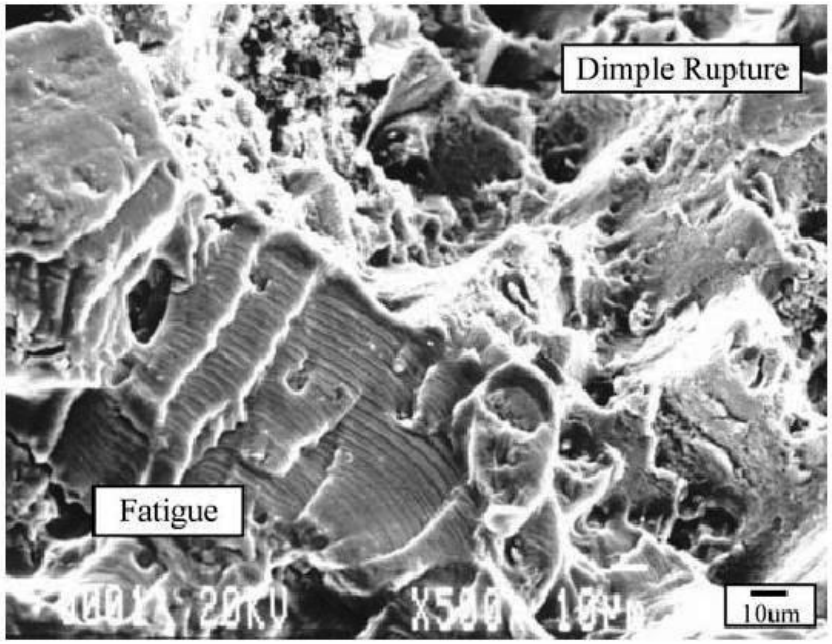

Fig. 9 Fatigue to dimpled rupture transition in 7075-T73

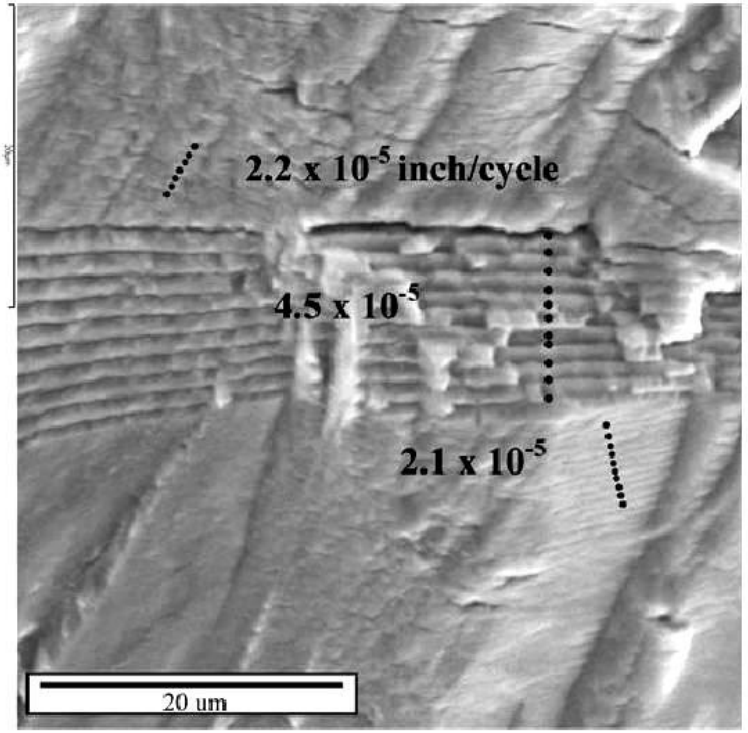

Fig. 22 Counting block or mixed load striations

Ref.: P.H. DeVries, K.T. Ruth, D.P. Dennies, **Counting on Fatigue : Striations and Their Measure**, "*J Failure Analysis and Prevention*," vol. 10, 2000, pp. 123, 130.

Fatigue Damage Accumulation Process

A schematic representation of the fatigue crack nucleation, initiation, and propagation phases is provided below.

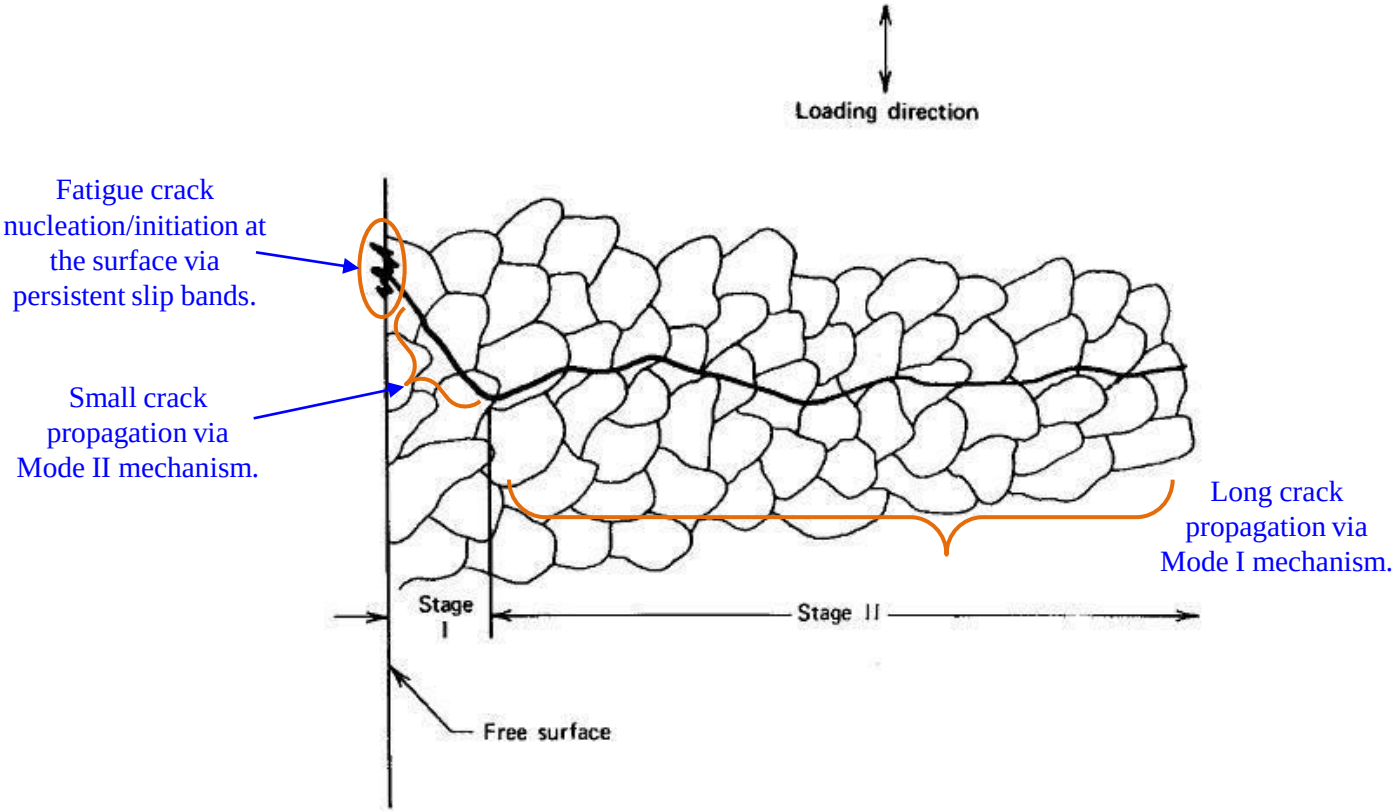

Figure 3.13 Schematic of stages I (shear mode) and II (tensile mode) transcrystalline microscopic fatigue crack growth.

Ref.: R. I. Stephens, A. Fatemi, R. R. Stephens, H. Fuchs, "**Metal Fatigue in Engineering, 2nd ed.,"** John Wiley & Sons, 2000, pp. 51.

S-N curve ; Fatigue Damage Accumulation

The cyclic time required to nucleate and initiate a fatigue crack consumes the majority of the overall fatigue life.

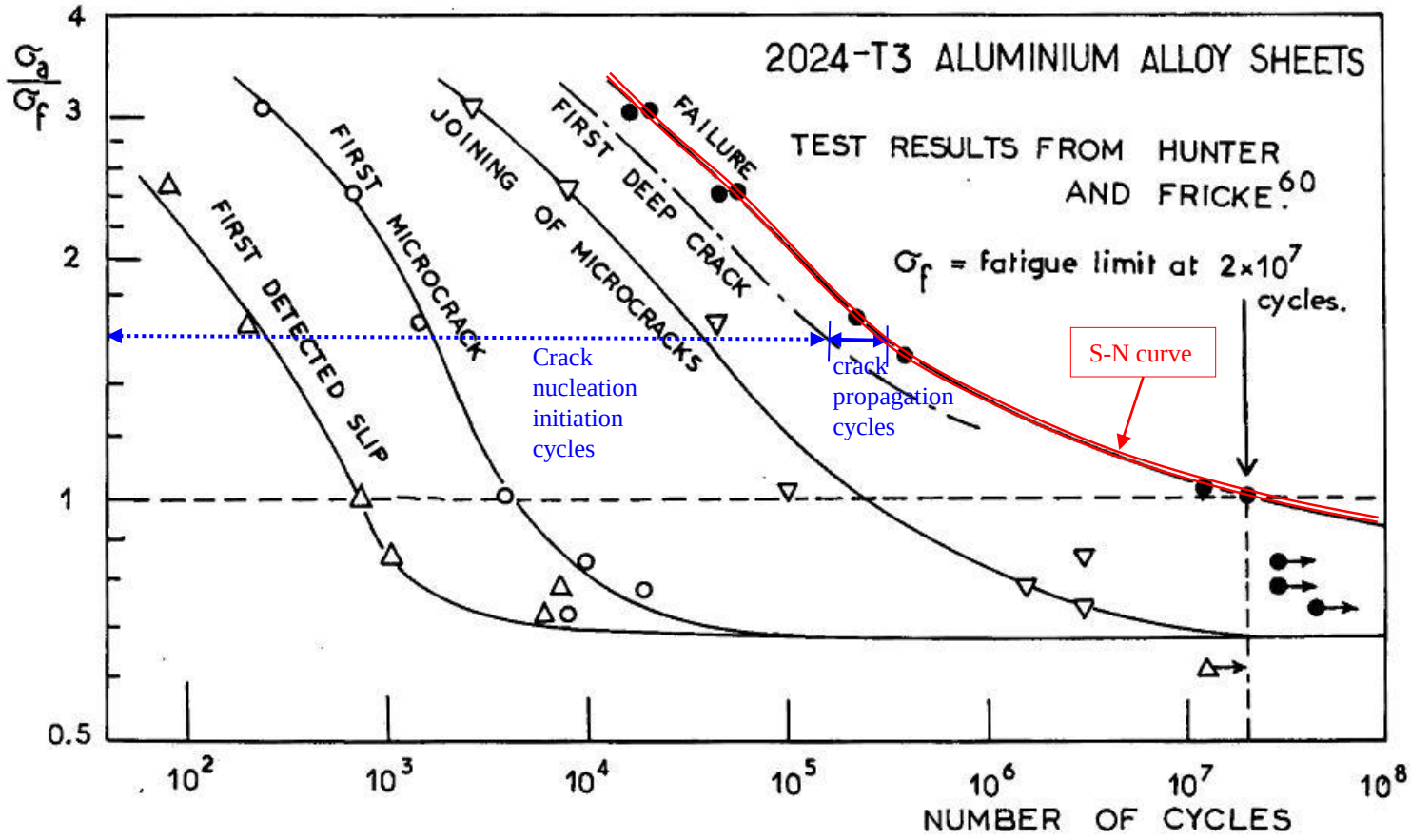

Fig. 5.42 Curves of stress versus number of cycles for first plastic slip, first microcrack, first joining of microcracks, first deep crack and failure

Ref. :W.G. Barrois, **Manual of Fatigue of Structures ; Fundamental and Physical Aspects**, AGARD-MAN-8-70, June 1970, pg 227.

S-N curve ; Fatigue Damage Accumulation (cont.)

The fatigue damage accumulation trend in terms of physical crack measurements with specialized equipment for various alloys is provided below.

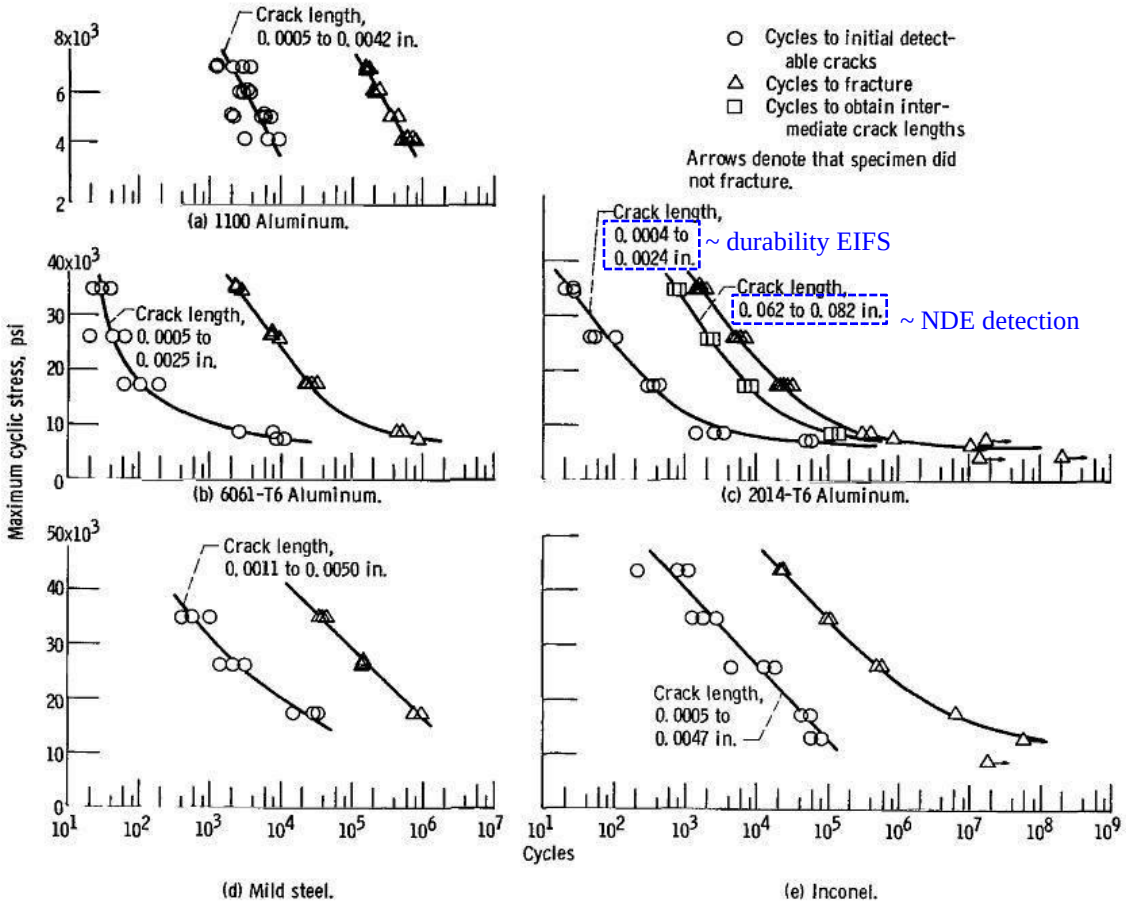

Figure 6. - Stress-life (S-N) curves showing cycles to first detectable cracks and cycles to fracture for center-notched sheet specimens. Ratio of minimum to maximum stress, 0.14.

NDE – non-destructive evaluation.
EIFS – equivalent initial flaw size

Ref. : S.J. Klima, D.J. Lesco, and J.C. Freche, **Ultrasonic Technique for Detection and Measurement of Fatigue Cracks**, NASA TN D-3007, 1965, pg 13.

S-N curve ; Fatigue Damage Accumulation (cont.)

The fatigue test results from full scale structure testing demonstrates the same trend observed at the coupon level.

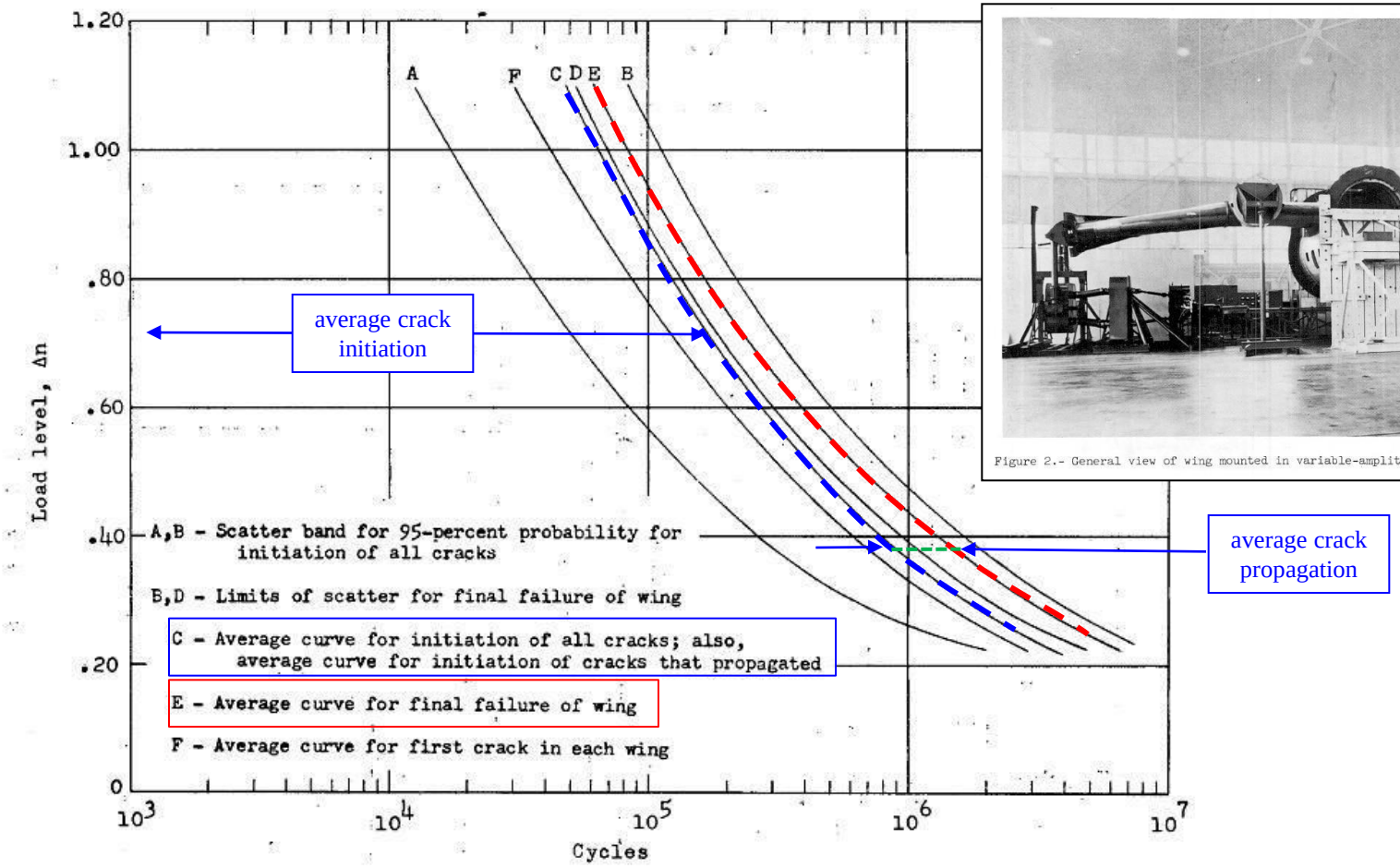

Figure 2.- General view of wing mounted in variable-amplitude fatigue machine. L-57-479.1

Figure 13.- Load-lifetime diagram from constant-amplitude tests.

Ref.: R.E. Whaley, **Fatigue Investigation of Full-Scale Transport Airplane Wings**, NACA TN 4132, 1957, pg 42.

Fatigue Failure Fracture Surface Features

Fatigue Failure Induced Surface Features

The information associated with a fracture surface (macroscopic and microscopic) typically affords useful details regarding the fundamental cause of the failure.

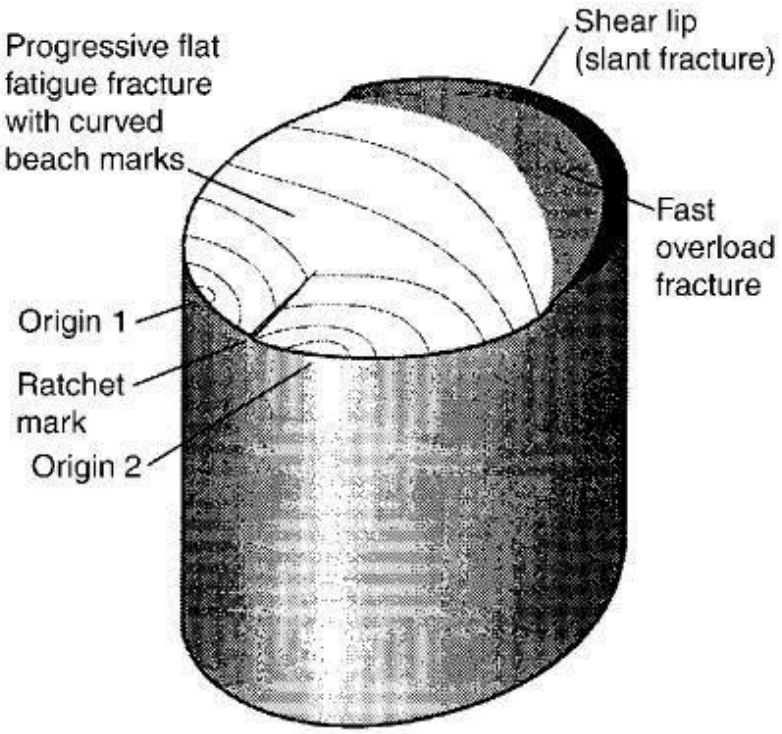

Fig. 1 General features of fatigue fractures.

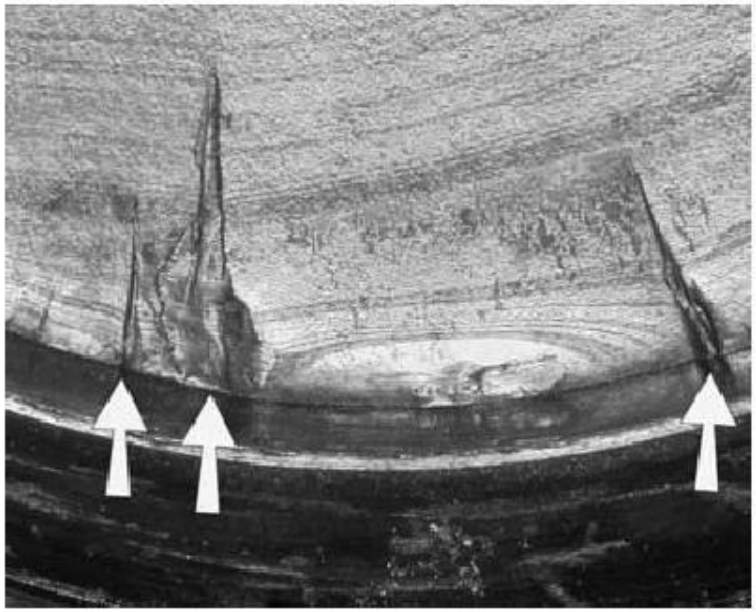

Fig. 2 Close-up view of ratchet marks between distinct surface origin sites in a low-alloy steel 18.4 cm (7.25 in.) shaft that failed in rotating bending fatigue. Ratchet marks (at arrows) are roughly radial steps formed where fatigue cracks initially propagating on different planes intersected. The ratchet mark at the middle arrow was damaged by postfracture contact.

Ref.: **ASM Handbook, Vol. 11 Failure Analysis Prevention**, R.A. Lund, ***Fatigue Fracture Appearances***, ASM International, 2002, pg. 627.

Fatigue Failure Induced Surface Features (cont.)

Macroscopic view of T-section fatigue failure.

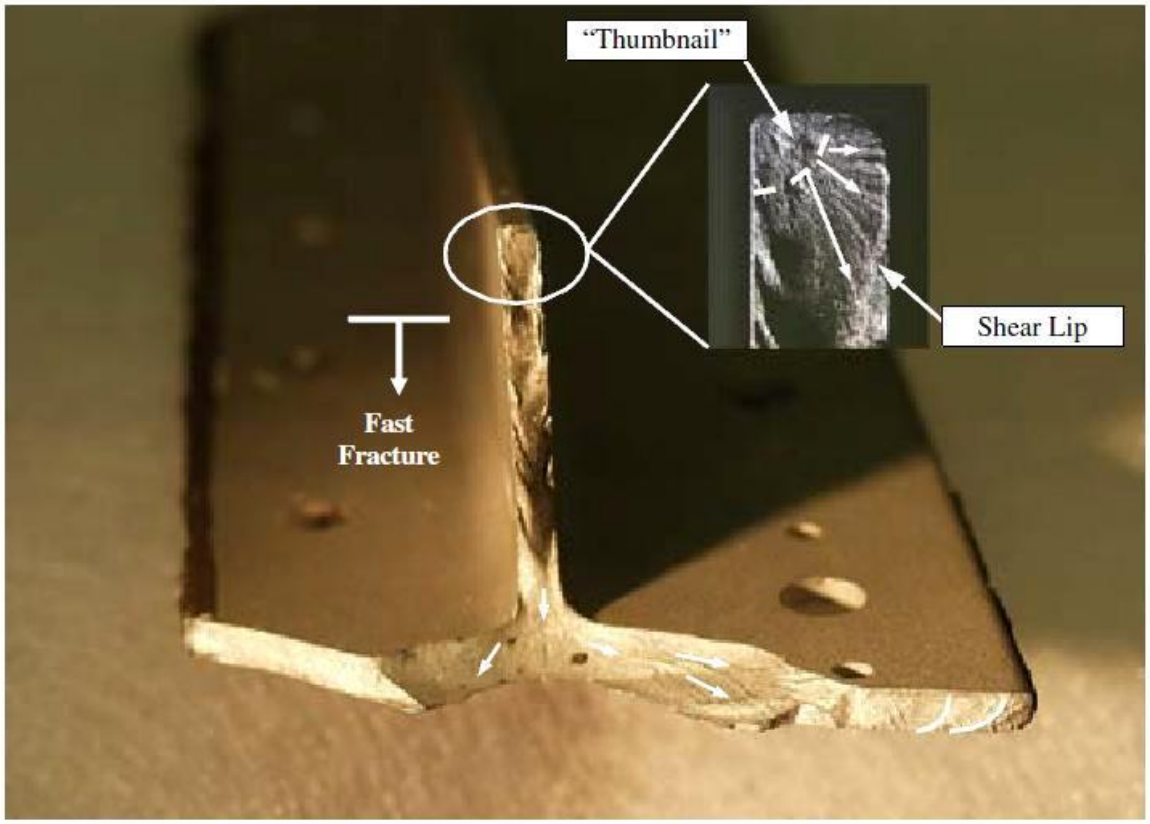

Fig. 26 Fracture obliterated by grit blast is evaluated from the overall fracture topography

Ref.: P.H. DeVries, K.T. Ruth, D.P. Dennies, **Counting on Fatigue : Striations and Their Measure**, "*J Failure Analysis and Prevention*," vol. 10, 2000, pg. 131.

Fatigue Failure Induced Surface Features (cont.)

Torsion fatigue in root of grooved bar. Fatigue crack initiation occurs on the surface via Mode III and Mode I propagation occurs in the circumferential direction (downhill) not radially.

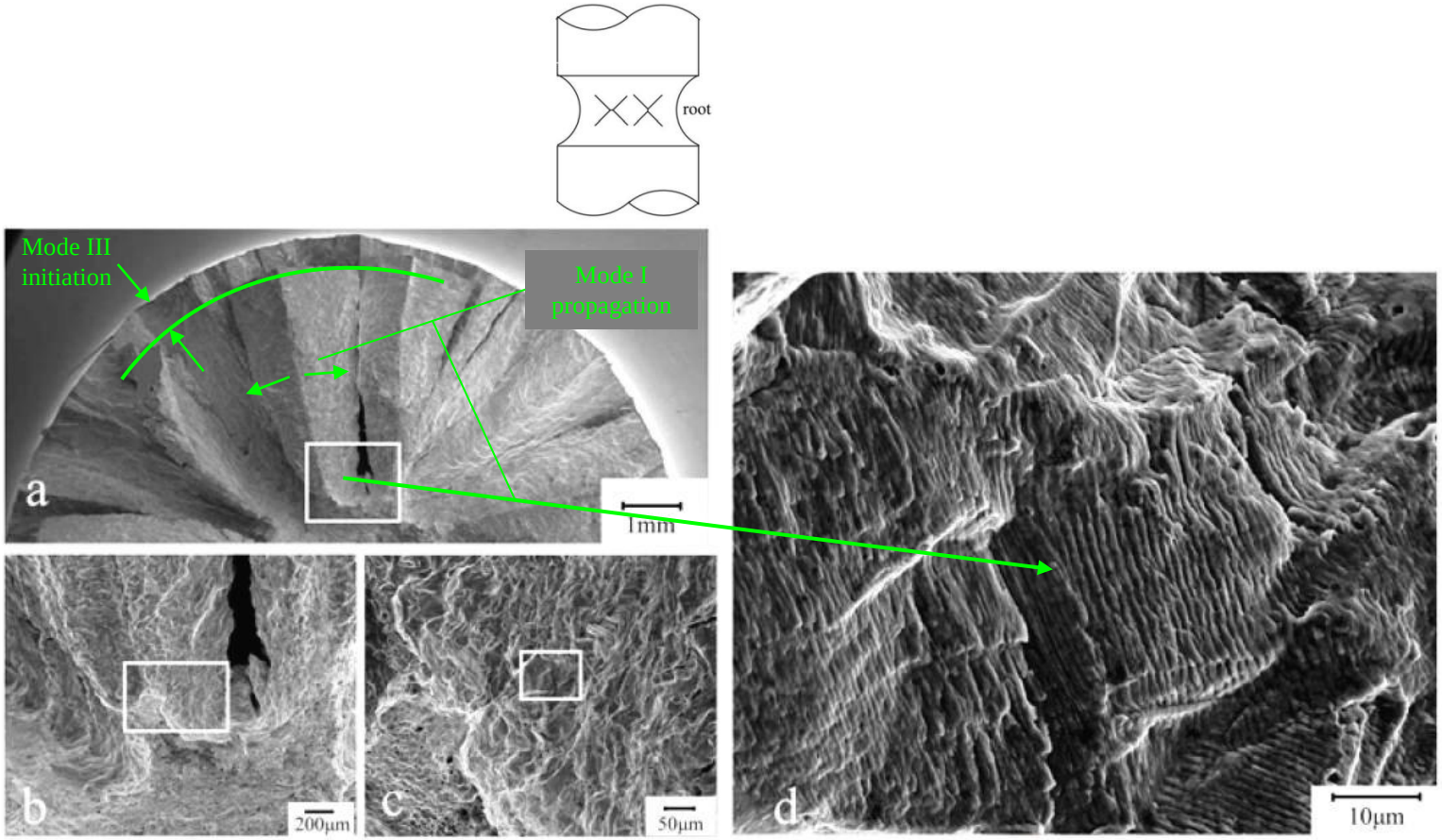

Fig. 10 Striation formed on factory-roof, NA, τ_a=180MPa, σ_m=0MPa.

Ref.: K. Tanaka, **Small Crack Propagation in Multiaxial Notch Fatigue**, pg 40, www.gruppofrattura.it/pdf/cp/CP2012005.pdf.

Fatigue Failure Fracture Surface Features (cont.)

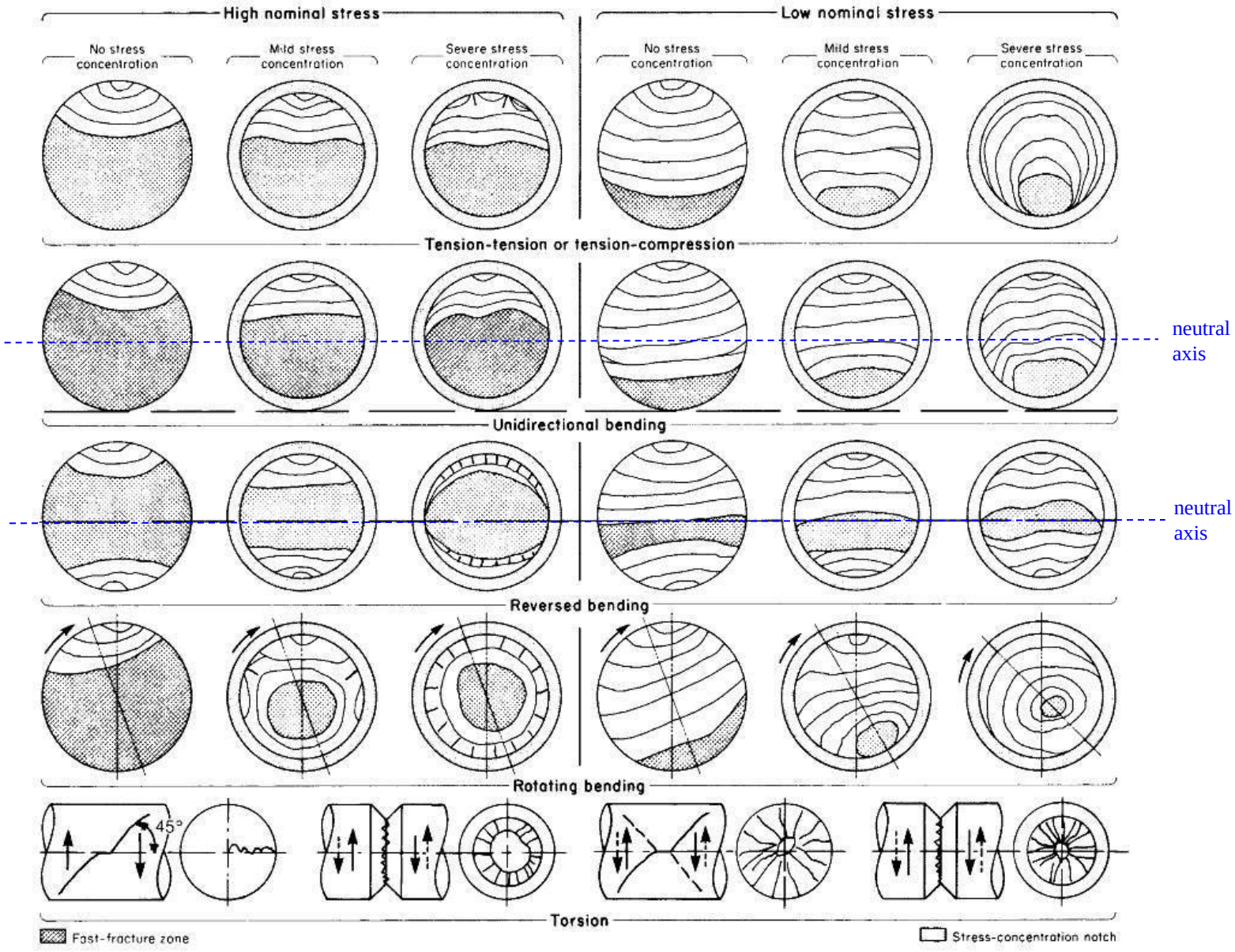

Fig. 25 Schematic diagrams illustrating characteristic patterns of fatigue beach marks, ratchet marks, and relative extent of fast overload fracture in cylindrical components subjected to various loading and notch conditions. Source: Ref 4

Ref.: **ASM Handbook, Vol. 11 Failure Analysis Prevention**, R.A. Lund, ***Fatigue Fracture Appearances***, ASM International, 2002, pg. 632.

Fatigue Failure Fracture Surface Features (cont.)

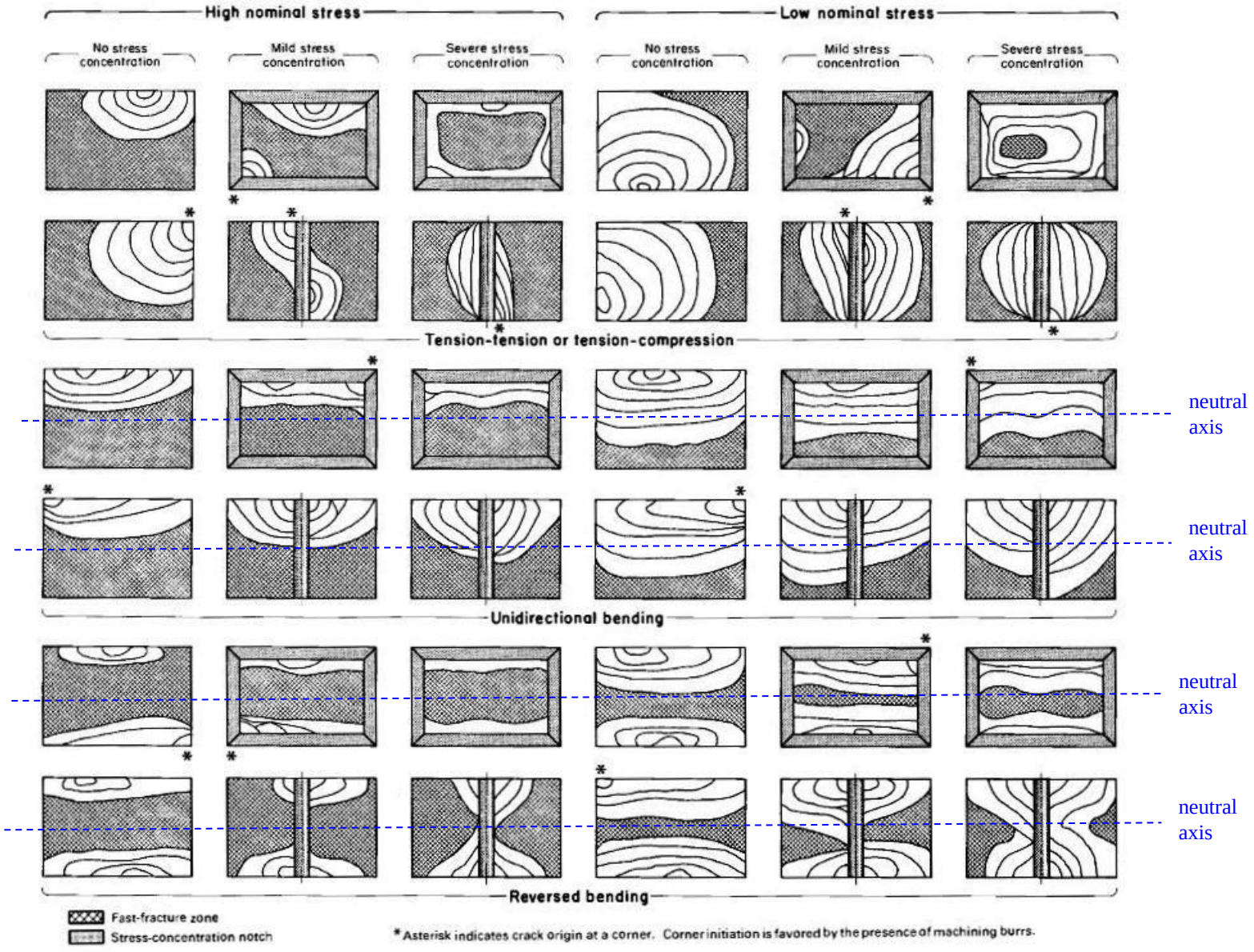

Fig. 49 Schematic representation of fatigue fracture surface marks produced in square and rectangular components and in thick plates under various loading conditions

Ref.: **ASM Handbook, Vol. 12 Fractography**, G.F. Vander Voort, ***Visual Examination and Light Microscopy***, ASM International, 1987, pg. 119.

Questions???

To Be Continued….

THANK YOU FOR ATTENDING…

Metal Fatigue Part 2

June 7, 1PM ET

Raymond Patin